

Panhandle polynomials of torus links and geometric applications

Andrei Mironov^{*1,2,3}, Hisham Sati^{†4,5}, Vivek Kumar Singh^{‡4}, and Alexander Stoimenov^{§6}

¹Lebedev Physics Institute, Moscow 119991, Russia.

²NRC Kurchatov Institute 123182, Moscow, Russia.

³Institute for Information Transmission Problems, Moscow 127994, Russia.

⁴Center for Quantum and Topological Systems (CQTS), NYUAD Research Institute, New York University Abu Dhabi, PO Box 129188, Abu Dhabi, UAE

⁵The Courant Institute for Mathematical Sciences, NYU, NY.

⁶Dongguk University, WISE campus, Department of Mathematics Education, 123, Dongdae-ro, 38066 Gyeongju-si, Republic of Korea

December 30, 2025

Abstract

We use a decomposition of the tensor of the fundamental representation of the quantum group $U_q(\mathfrak{sl}_N)$ and the Rosso-Jones formula to establish a peculiar “panhandle” shape of the HOMFLY-PT polynomial of the reverse parallel of torus knots and links. Due to their panhandle-like intrinsic properties, the HOMFLY-PT polynomial is referred to as a “panhandle polynomial”. With the help of the ℓ -invariant, this extends to links the Etnyre-Honda result about the arc index and maximal Thurston-Bennequin invariant of torus knots. It has further geometric consequences, related to the braid index, the existence of minimal string Bennequin surfaces for banded and Whitehead doubled links, the Bennequin sharpness problem, and the equivalence of their quasipositivity and strong quasipositivity. We extend these properties to torus links, which relate to the classification of their component-wise Thurston-Bennequin invariants. Finally, we discuss the definition of the ℓ -invariant for general links.

^{*}mironov@itep.ru

[†]hsati@nyu.edu

[‡]vks2024@nyu.edu

[§]stoimenov@stoimenov.net

Contents

1	Introduction	3
2	Panhandle polynomials for torus knots and links	4
2.1	Background and Definitions	4
2.2	HOMFLY-PT polynomial of reverse 2-cable torus knot $T(m, n)$	7
2.3	Proof of the Panhandle theorem for torus knots	13
2.4	Extension to torus links	15
3	Geometric properties	18
3.1	Arc index and Thurston-Bennequin invariant	18
3.2	Braid index and braided surfaces	19
3.3	Quasipositivity and strong quasipositivity	20
3.4	Properties of torus knots	21
4	Applications to torus links	23
4.1	Invariants	23
4.2	Geometric properties	29
4.3	Whitehead doubled links	35
4.4	Generalizing the ℓ -invariant for arbitrary links	35

1 Introduction

Polynomial invariants have provided deep insights into knot theory and topology. Some of the most widely studied knot polynomial invariants include the Alexander polynomial [Al], the Jones polynomial [Jo], and the HOMFLY-PT polynomial [H+]. In this paper, we exhibit a peculiar shape of the latter polynomial of the reverse parallel of a torus knot and a torus link. We fix for $K = T_{m,n} = T(m,n)$, with

$$(m,n) = 1, \quad m < n,$$

the vertical framing $t = t_v$, given in (3), and the convention (5) below. Our main result is the following:

Theorem 1.1 (Panhandle Theorem). *Let $X = [\underline{M}; M]_v$ denote a polynomial such that*

$$\min \deg_v X = \underline{M} \quad \text{and} \quad \max \deg_v X = M. \quad (1)$$

Then the HOMFLY-PT polynomial for the reverse 2-cable torus knot $C_2(T_{m,n}, t)$ has the form

$$P(C_2(T_{m,n}, t)) = [1 - 2m; 2m - 1]_v + \underbrace{(m-1)zv \frac{v^{2n} - v^{2m}}{v^2 - 1}}_{\text{panhandle}}.$$

The condition $m < n$ is essential: restoring the symmetry of the torus knot $T(m,n)$ in m and n (topological framing) requires the vanishing of certain leading coefficients in the Laurent polynomial $[1 - 2m; 2m - 1]_v$ when $m > n$.

Establishing Theorem 1.1 directly from the skein relation (5) is cumbersome. Hence, we adopt a representation theory approach. The construction of HOMFLY-PT invariants, denoted by $\mathcal{H}(C_2(T_{m,n}, t))$, naturally relies on the decomposition of the tensor product of representations (see [RT][MMM2]) into irreducible components

$$R \otimes \bar{R} = \bigoplus_i Q_i, \quad Q_i \in \text{Rep}(U_q(\mathfrak{sl}_N)).$$

Here R denotes the fundamental representation associated with a Young tableau of the quantum group $U_q(\mathfrak{sl}_N)$ and \bar{R} is its conjugate. In this context, the HOMFLY-PT polynomial of a knot $C_2(T_{m,n}, t)$ can be written as the sum of contributions from the relevant representations, namely the scalar representation ($Q_1 = \Phi$) and the adjoint representation ($Q_2 = \text{Adj}$):

$$P(C_2(T_{m,n}, t_v)) := \mathcal{H}(C_2(T_{m,n}, t_v)) = \frac{1}{\mathcal{H}_R(U)} \left(\mathcal{H}_\Phi(T_{m,n}) + \mathcal{H}_{\text{Adj}}(T_{m,n}) \right). \quad (2)$$

Here

$$t_v = (1 - m)n \quad (3)$$

is the vertical framing (see Defs. 2.3 and 2.10) and U is the unknot. Whereas the HOMFLY-PT polynomial of the scalar representation $\mathcal{H}_\Phi(K) = 1$, that of the adjoint representation $\mathcal{H}_{\text{Adj}}(K)$ is generally nontrivial. This formulation provides a natural framework for analyzing the structure of $P(C_2(T_{m,n}, t))$. Theorem 1.1 emerges from expression (2) using the Rosso-Jones formula ([LZ, Theorem 5.1][RJ, Theorem 8]), which provides a systematic approach to understanding the adjoint polynomials of torus knots $\mathcal{H}_{\text{Adj}}(T_{m,n})$. We describe this in §2, with a general proof of Theorem 1.1 established in §2.3. The particular case of $m = 2$ of Theorem 1.1 was proved in [JLS2] by the fourth author using skein algebra programming. The leading (v -degree) term of the panhandle for $m = 2$ was also identified by Diao and Morton [DM, Theorem 2.7].

The main motivation behind Theorem 1.1 is not the peculiar shape of the polynomial. It emerged through explicit computations related to very different subjects. Specifically, it is related to a new method of estimating the arc index and maximal Thurston-Bennequin invariant of knots [JLS2]. This method, which relies on a quantity named ℓ -invariant, allows for an algebraic proof of some of Etnyre-Honda's work [EH] on torus knots. The work in [JLS2] allows us to further relate to the braid index of the reverse parallel (see [DM]), the existence of its minimal

string Bennequin surfaces (see [BMe][HS]), the Bennequin sharpness problem (Problem 3.8), and the equivalence of quasipositivity and strong quasipositivity for certain links. We outline these applications in §3.

Theorem 1.1 also admits an extension to the setting of torus links, which we discuss in §2.4. This extension follows directly from the underlying Def. 2.32 and the arguments developed in §2.4. We state the result in the following theorem (see Theorem 2.34).

Theorem 1.2 (Panhandle for links). *The HOMFLY-PT polynomial for the reverse 2-cable l -component torus link $C_2(T_{m,n}, t_v)$ has the form*

$$P(C_2(T_{m,n}, t_v)) = \left[1 - 2m; 2n \frac{l-1}{l} + \frac{2m}{l} - 1 \right]_v + \underbrace{\zeta_{m,l} z v \frac{v^{2n} - v^{2m}}{v^2 - 1}}_{\text{panhandle}},$$

where

$$\zeta_{m,l} := \sum_{k=0}^l (-1)^{l+k} \frac{l!}{(l-k)!} \left(\frac{m}{l} \right)^k.$$

Hence, the length of the link panhandle is equal to $2(n-m)/l$.

In §4 we extend the above applications to torus links. Apart from determining their arc index, we give a full description of their component-wise Thurston-Bennequin invariants in §4.1.2. Then, the further geometric applications outlined for torus knots are largely generalized to torus links in §4.2, with the addition of the Baker-Motegi problem (§4.2.4). The conclusion of §4 (and the paper) discusses the extension of the ℓ -invariant for general links, based on the properties studied for the torus links.

2 Panhandle polynomials for torus knots and links

2.1 Background and Definitions

Definition 2.1 (Torus Knots). Let $m, n \in \mathbb{Z}_{>0}$ such that $\gcd(m, n) = 1$. The *torus knot* $T_{m,n} = T(m, n)$ is defined as the closure of the braid word

$$T_{m,n} := \widehat{(\sigma_1 \sigma_2 \cdots \sigma_{m-1})^n} \in B_m,$$

where B_m is the braid group on m strands with standard Artin generators $\sigma_1, \dots, \sigma_{m-1}$. The closure operation, $\widehat{\cdot}$, connects the corresponding top and bottom endpoints of the braid to form a knot.

Example 2.2. The torus knot $T_{4,3}$ is the closure of the braid $(\sigma_1 \sigma_2 \sigma_3)^3 \in B_4$. See Fig. 1 for an illustration.

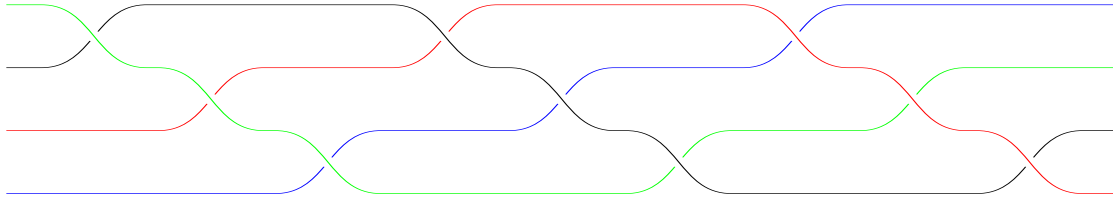


Figure 1: Braid representation of torus knots $T(4,3)$.

Definition 2.3 (The reverse 2-cable knots). Let $K = \widehat{\beta}$ be the closure of a braid $\beta \in B_m$. Define the *reverse 2-cable* of β to be the braid $\phi(\beta) \in B_{2m}$ obtained by “doubling and reversing orientation” of each strand of β with framing t . The framing $t \in \mathbb{Z}$ is defined by the factor of $q^{t\kappa_\lambda}$ (see (10)) that differs the framed HOMFLY-PT polynomial from the invariant polynomial (topological framing). The sign of framing changes if the orientation is reversed. We will use the vertical framing [AM], which for the torus knot $T(m, n)$ is given in (3). Concretely, on the Artin generators

$$\phi : B_m \longrightarrow B_{2m}, \quad \phi(\sigma_i) = \sigma_{2i} \sigma_{2i+1} \sigma_{2i-1} \sigma_{2i} \quad (1 \leq i \leq m-1). \quad (4)$$

Then the *2-cable knot* $C_2(K, t)$ is

$$C_2(K, t) := \widehat{\phi(\beta)} \in S^3.$$

See Fig. 2 for a schematic of the *reverse 2-cable torus knot* $T_{4,5}$ with framing $t = -15$.

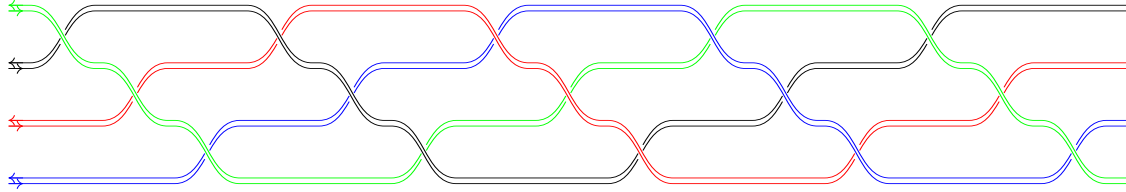


Figure 2: Braid representation of reverse 2-cable torus knots $T_{4,5}$.

Definition 2.4 (HOMFLY-PT Polynomial[H+]). For a knot K , the (uncolored) *HOMFLY-PT polynomial* $P(K)$ is defined via the skein relation (Morton convention):

$$v^{-1}P(L_+) - vP(L_-) = zP(L_0), \quad P(U) = 1. \quad (5)$$

Here, U denotes the unknot (trivial knot), and $z = q - q^{-1}$.

As highlighted in the Introduction, we focus on studying the HOMFLY-PT polynomial of *reverse 2-cable torus knots* and its geometric applications. Directly applying the skein relations (see Def. 2.4) can be quite complex in general. Therefore, we address the problem through representation theory[RT], focusing on the R -colored HOMFLY-PT invariants $H_R(K)$, where the Young tableau R corresponds to a representation of $U_q(\mathfrak{sl}_N)$ (see Def. 2.6). In particular, when $R = [1]$ (the fundamental representation), the invariant reduces to the usual HOMFLY-PT polynomial (5), i.e.,

$$H_{[1]}(K) = H(K) = P(K).$$

Remark 2.5 (Normalizations). There are two normalizations of the HOMFLY-PT polynomial: the normalized (reduced) polynomial such that $H_R(U) = 1$ where U denotes the unknot (trivial knot), and the un-normalized (unreduced) polynomial. We use the notation H_R and \mathcal{H}_R correspondingly in these two cases so that, for the knot K , $\mathcal{H}_R(K) = \mathcal{H}_R(U) \cdot H_R(K)$, and similarly for polynomials $P(K)$.

Definition 2.6 (Young tableau diagram representation [KR][KS]). A representation R of the quantum group $U_q(\mathfrak{sl}_N)$ ($|q| < 1$) with highest weight Λ can be uniquely specified by a Young tableau

$$R = [R_1, R_2, \dots, R_{N-1}], \quad R_1 \geq R_2 \geq \dots \geq R_{N-1} \geq 0. \quad (6)$$

If the highest weight is expressed as

$$\Lambda_R = \sum_{i=1}^{N-1} a_i \omega_i, \quad (7)$$

with fundamental weights $\{\omega_i\}_{i=1}^{N-1}$, then the Young tableau entries in (6) relate to the coefficients a_i in (7) by

$$R_i = \sum_{j=i}^{N-1} a_j, \quad \text{for } i = 1, \dots, N-1.$$

For general N , the conjugate representation \bar{R} corresponds to the highest weight

$$\Lambda_{\bar{R}}^* := \sum_{i=1}^{N-1} a_{N-i} \omega_i,$$

which is associated to the conjugate Young tableau.

Definition 2.7 (Composite representation [Ko]). The composite representation is the most general finite-dimensional irreducible highest weight representation of \mathfrak{sl}_N , which is associated with the Young diagram of the form

$$(R, P) = \left[R_1 + P_1, \dots, R_{l_R} + P_1, \underbrace{P_1, \dots, P_1}_{N-l_R-l_p}, P_1 - P_{l_p}, P_1 - P_{l_p-1}, \dots, P_1 - P_2 \right],$$

where l_P denotes the number of lines in the Young diagram P . This (R, P) is the first (“maximal”) representation, contributing to the product $R \otimes \bar{P}$. It can be manifestly obtained from the tensor products (i.e., as a projector from $R \otimes \bar{P}$) by formula [Ko]

$$(R, P) = \sum_{Y, Y_1, Y_2} (-1)^{l_Y} N_{YY_1}^R N_{Y^T Y_2}^P Y_1 \otimes \bar{Y_2}, \quad (8)$$

where the superscript “T” denotes transposition of Young diagram.

Example 2.8 (Fundamental representation). The Young tableau diagrams for the fundamental representation $R = [1]$ and its conjugate $\bar{R} = [\bar{1}]$ of $U_q(\mathfrak{sl}_N)$ are given by

$$[1] = \square \quad \text{and} \quad [\bar{1}] = \underbrace{[1, 1, \dots, 1]}_{N-1} = [1^{N-1}] = \left. \begin{array}{c} \square \\ \vdots \\ \square \end{array} \right\} N-1.$$

Here, $[\bar{1}]$ can be viewed as a composite representation $(\Phi, [1])$, with Φ the trivial representation.

Example 2.9 (Adjoint representation). Another simple example is the adjoint representation of $U_q(\mathfrak{sl}_N)$:

$$\text{Adj} = ([1], [1]) = [2, \underbrace{1, \dots, 1}_{N-2}] = [2, 1^{N-2}] = \left. \begin{array}{c} \square \\ \vdots \\ \square \end{array} \right\} N-1.$$

Definition 2.10 (HOMFLY-PT polynomial for $C_2(K, t)$). Let K be a knot, and let $\mathcal{H}_R(K)$ denotes the R -colored HOMFLY-PT polynomial of K colored by a Young tableaux representation R of the group $U_q(\mathfrak{sl}_N)$. Given

$$R \otimes \bar{R} = \bigoplus_i Q_i,$$

with each $Q_i \in \text{Rep}(U_q(\mathfrak{sl}_N))$, the R -colored HOMFLY-PT polynomial (un-normalized) of the *reverse 2-cable knot* (which is a link) denoted $C_2(K, t)$ is given by

$$\mathcal{H}_R(C_2(K, t_v)) := \sum_i \mathcal{H}_{Q_i}(K).$$

In particular, for the fundamental representation (the simplest representation), i.e. $R = [1]$, we have

$$R \otimes \bar{R} = \Phi \oplus \text{Adj},$$

where Φ denotes the trivial representation and $\text{Adj} = [2, 1^{N-2}]$ denotes the adjoint representation of $U_q(\mathfrak{sl}_N)$. Therefore, the fundamental normalized HOMFLY-PT polynomial of the reverse 2-cable knot is

$$P(C_2(K, t_v)) = \frac{1}{\mathcal{H}_{[1]}(U)} (\mathcal{H}_\Phi(K) + \mathcal{H}_{\text{Adj}}(K)), \quad (9)$$

where $\mathcal{H}_\Phi(K) = 1$, and $\mathcal{H}_{\text{Adj}}(K)$ denotes the HOMFLY-PT polynomial of knot K in the adjoint representation.

Remark 2.11 (The vertical framing). As any formula of representation theory origin, this formula is correct only when the polynomials are in the vertical framing [AM]. Hence, throughout the paper, all HOMFLY-PT polynomials are assumed to be in the vertical framing.

Remark 2.12 (Uniform HOMFLY-PT polynomial). The HOMFLY-PT polynomial colored by a (fixed) representation R (Young diagram) is a Laurent polynomial in q and v , which under the specialization $v = q^N$ reduces to the \mathfrak{sl}_N invariant $J_R^{\mathfrak{sl}_N}(q)$. For the adjoint representation, $R_N = [2, 1^{N-2}]$ as above, so that the color R is specifically correlated with v . We define $H_{\text{Adj}}(K)$ via the specialization

$$H_{\text{Adj}}(K) \Big|_{v=q^N} = J_{[2, 1^{N-2}]}^{\mathfrak{sl}_N}(q),$$

for all sufficiently large N [ChE][HM]. This polynomial is called *uniform HOMFLY-PT polynomial* in [MMM], and the same construction applies to any composite representation.

Note that Eq. (9) provides the HOMFLY-PT polynomial for the knot $C_2(K, t_v)$, consistent with the skein relation in Def. 2.4. Moreover, we would like to emphasize that working with Eq. (9) is more convenient than using the skein relations.

Notation 2.13. Throughout this article, we use the following shorthand $[x]_q$ for the q -number and $\{x\}$ for the antisymmetric bracket

$$[x]_q = \frac{q^x - q^{-x}}{q - q^{-1}}, \quad \{x\} = x - \frac{1}{x},$$

In particular, we set $z = \{q\}$.

In the following subsections, we present a detailed study of the HOMFLY-PT polynomial of *reverse 2-cable torus knots* $C_2(T(m, n), t)$ in the vertical framing, and then extend to torus links.

2.2 HOMFLY-PT polynomial of reverse 2-cable torus knot $T(m, n)$

To evaluate the HOMFLY-PT polynomial of the knot $C_2(K, t_v)$, we first compute the adjoint HOMFLY-PT polynomial for the knot K . To that end, we first review the quantum dimensions of Young diagram representation R . These quantum dimensions and their properties are associated with the knot K . See [KS][KRT].

Definition 2.14 (The quantum dimension of representation R). For the Young diagram R , introduce a function of two variables q and v labeled by R :

$$D_R(q, v) := \prod_{i,j \in R} \frac{\{vq^{j-i}\}}{\{q^{h(i,j)}\}}$$

where $h(i, j)$ is the hook length, and the product runs over boxes of the Young diagram. Letting R be a Young diagram associated with the representation of the quantum group $U_q(\mathfrak{sl}_N)$, the quantum dimension of this representation is defined to be $D_R(q, q^N)$.

Example 2.15 (Quantum dimension of the adjoint). $R = [2, 1] = \begin{smallmatrix} & & \\ & \square & \\ \square & & \end{smallmatrix}$ is a Young diagram of length $|R| = 3$. Then

$$D_{[2,1]}(q, v) = \frac{v - v^{-1}}{q^3 - q^{-3}} \cdot \frac{vq - v^{-1}q^{-1}}{q - q^{-1}} \cdot \frac{vq^{-1} - v^{-1}q}{q - q^{-1}},$$

where the hook lengths are $h(1, 1) = 3$, $h(1, 2) = 1$, and $h(2, 1) = 1$. This representation is adjoint at $N = 3$. At generic N , the adjoint representation is $R = \text{Adj} = [2, 1^{N-2}]$, i.e.,

$$D_{[2, 1^{N-2}]} = \frac{\{q^{N-1}\}}{\{q\}} \cdot \prod_{i=1}^N \frac{\{q^{2-i}v\}}{\{q^i\}},$$

so that the adjoint quantum dimension, after choosing $v = q^N$, is

$$D_{\text{Adj}} = \frac{\{vq\}\{v/q\}}{\{q\}^2}.$$

Remark 2.16 (Properties of quantum dimension). $D_R(q, v)$ is a rational function of q and v , and satisfies the following properties:

- (i) $D_R(q, v) = D_R(q^{-1}, v^{-1})$,
- (ii) $D_R(q^{-1}, v) = D_{R^T}(q, v)$,
- (iii) $D_R(q, v) = v^{|R|} q^{c(R)} A_R(q) + \cdots + (-1)^{|R|} v^{-|R|} q^{-c(R)} A_R(q)$,

where R^T denotes the transpose of Young diagram R , $c(R) = \sum_{(i,j) \in R} (j-i)$, and $A_R(q) = \prod_{(i,j) \in R} \{q^{h(i,j)}\}^{-1}$.

Note that Property (iii) holds when the length of the Young diagram representation R , i.e. the partition length $|R|$, is independent of the rank of the group N .

Remark 2.17 (Properties of the unknot polynomials). The quantum dimension of R is equal to the unknot HOMFLY-PT polynomial colored with R , $\mathcal{H}_R(U; q, v) = D_R(q, v)$, i.e., $\mathcal{H}_R(K) = D_R(q, v) \cdot H_R(K)$. Hence, the three properties in Remark 2.16 characterize the HOMFLY-PT polynomial of the unknot.

Remark 2.18 (Properties of HOMFLY-PT polynomial). Generally, under reversal of parameters, the HOMFLY-PT polynomial of knot K transforms as

$$\begin{aligned} H_R(K) &\xrightarrow{q \mapsto q^{-1}, v \mapsto v^{-1}} H_R(!K), \\ H_R(K) &\xrightarrow{q \mapsto q^{-1}} H_{R^T}(K), \end{aligned}$$

where $H_R(!K)$ denotes the polynomial of the mirror-reflected knot $!K$.

Now, we turn to the discussion of adjoint polynomials of knots, with a particular focus on torus knots $T(m, n)$. The Rosso-Jones formula for the colored HOMFLY-PT invariants of torus knots is stated in the following theorem ([LZ, Theorem 5.1][RJ, Theorem 8]).

Theorem 2.19. *Let K be the torus knot $T(m, n)$, where m and n are relatively prime. Let $R \vdash s$ be a partition. Then the reduced colored HOMFLY-PT polynomial in the vertical framing is given by:*

$$\mathcal{H}_R(K) = q^{n\kappa_R} \cdot \sum_{\mu \vdash m \text{ } s} c_\mu^R \cdot q^{-n\kappa_\mu/m} \cdot D_\mu(q, v),$$

where

- $v = q^N$,
- $\kappa_R = (\Lambda_R, \Lambda_R + 2\rho)$ is the eigenvalue of the quadratic Casimir operator in the representation μ of \mathfrak{sl}_N ,

$$\kappa_R = 2 \sum_{i,j \in R} (j-i) - \frac{s^2}{N} + sN, \quad (10)$$

- ρ is the Weyl vector,
- and c_μ^R are the integers determined by the Adams operation (m-plethystic expansion):

$$\widehat{Ad}_m S_R(x_1, x_2, \dots) := S_R(x_1^m, x_2^m, \dots) = \sum_{\mu \vdash m \text{ } s} c_\mu^R \cdot s_\mu(x_1, x_2, \dots).$$

This formula allows explicit computation of the colored HOMFLY-PT polynomial for torus knots.

Remark 2.20 (Conventions). We added a factor of $q^{-(m-1)n\kappa_R}$ as compared with the formula for $\mathcal{H}_R(K)$ in [LZ, Theorem 5.1][RJ, Theorem 8] (where the polynomial is in the topological framing) since we need the polynomials in the vertical framing in order to deal with formula (9). This exponent $-(m-1)n\kappa_R$ in this factor is the number $(m-1)n$ of Artin generators σ_i giving the torus knot in Definition 2.1, each of them being associated with the inverse \mathfrak{R} -matrix (hence, the sign minus), and q^{κ_R} emerges due to the difference in normalization of these generators in the topological and vertical framings.

Remark 2.21 (Consistency). The HOMFLY-PT polynomial in Theorem 2.19 corresponds to the Reshetikhin-Turaev invariant [D+] constructed from the inverse R -matrices, which are associated with the mirror knot. This corresponds to the replacement $v \rightarrow v^{-1}$, $q \rightarrow q^{-1}$ in the invariant. At the same time, the skein relation (5) is associated with just the replacement $v \rightarrow v^{-1}$. However, as soon as we are interested in the adjoint representation, and its polynomial is invariant with respect to the replace $q \rightarrow q^{-1}$, the skein relation is consistent with Theorem 2.19.

Applying Theorem 2.19, we can deduce the HOMFLY-PT polynomial for reverse 2-cable torus knot. The subsequent subsections discuss the details.

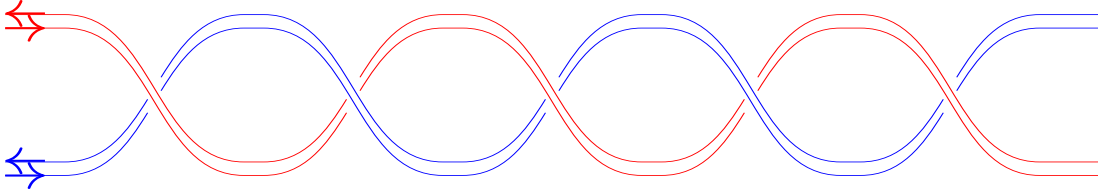


Figure 3: Braid representation of $C_2(T_{2,5}, -10)$.

Example 2.22 (HOMFLY-PT polynomial of reverse 2-cable torus knot $T(2, n)$). The adjoint polynomials for torus knot $T_{2,n}$, as stated in Theorem 2.19, can be computed explicitly [MMM]:

$$\mathcal{H}_{\text{Adj}}(T_{2,n}) = v^{2n} - D_{([1,1],[2])}(q, v) - D_{([2],[1,1])}(q, v) + q^{-2n} D_{([2],[2])}(q, v) + q^{2n} D_{([1,1],[1,1])}(q, v).$$

Here

$$\begin{aligned} D_{([2],[2])}(q, v) &= \frac{\{v\}^2 \{vq^3\} \{v/q\}}{\{q^2\}^2 \{q\}^2}, & D_{([1,1],[1,1])}(q, v) &= \frac{\{vq\} \{v\}^2 \{v/q^3\}}{\{q^2\}^2 \{q\}^2}, \\ D_{([1,1],[2])} &= D_{([2],[1,1])}(q, v) = \frac{\{vq^2\} \{vq\} \{v/q^2\} \{v/q\}}{\{q^2\}^2 \{q\}^2}. \end{aligned}$$

Using the result of Eq. (9), we then obtain the HOMFLY-PT polynomial of $C_2(T_{2,n}, -n)$

$$P(C_2(T(2,n), -n)) = \frac{1}{D_{[1]}} (1 + \mathcal{H}_{\text{Adj}}(T_{2,n})),$$

where

$$D_{[1]} = \frac{(-1 + v^2)}{(vz)} = \frac{\{v\}}{\{q\}}.$$

For illustration purposes, we present selected examples in Tables 1 and 2, with their associated geometric properties.

$(z \setminus v)$	-3	-1	1	3	5	7	9
-1	-9	21	-16	4	0	0	0
1	-24	71	-50	5	1	1	1
3	-22	84	-63	1	0	0	0
5	-8	45	-37	0	0	0	0
7	-1	11	-10	0	0	0	0
9	0	1	-1	0	0	0	0

Table 1: HOMFLY-PT Polynomial of $C_2(T_{2,5}, -5)$ knot; the yellow box highlights a panhandle-like structure.

$(z \setminus v)$	-3	-1	1	3	5	7	9	11	13	15	17	19	21
-1	-36	96	-85	25	0	0	0	0	0	0	0	0	0
1	-420	1131	-910	201	1	1	1	1	1	1	1	1	1
3	-1897	5319	-4032	610	0	0	0	0	0	0	0	0	0
5	-4352	13237	-9805	920	0	0	0	0	0	0	0	0	0
7	-5776	19678	-14673	771	0	0	0	0	0	0	0	0	0
9	-4744	18643	-14275	376	0	0	0	0	0	0	0	0	0
11	-2486	11642	-9262	106	0	0	0	0	0	0	0	0	0
13	-832	4846	-4030	16	0	0	0	0	0	0	0	0	0
15	-172	1330	-1159	1	0	0	0	0	0	0	0	0	0
17	-20	231	-211	0	0	0	0	0	0	0	0	0	0
19	-1	23	-22	0	0	0	0	0	0	0	0	0	0
21	0	1	-1	0	0	0	0	0	0	0	0	0	0

Table 2: HOMFLY-PT Polynomial of $C_2(T_{2,11}, -11)$.

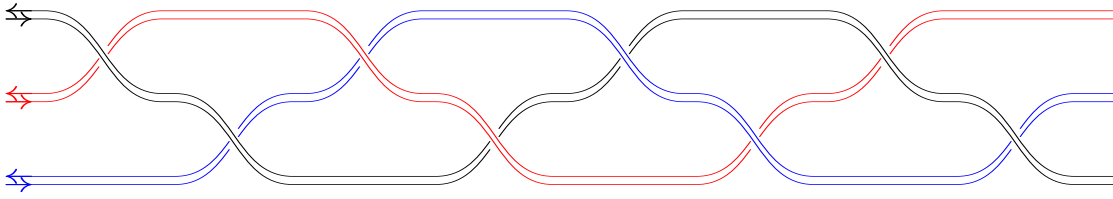


Figure 4: Braid representation of reverse two-cable torus knot $C_2(T_{3,4}, -8)$.

Example 2.23 (HOMFLY-PT polynomial of reverse 2-cable torus knot $T(3, n)$). According to Theorem 2.19, the adjoint polynomials associated with a torus knot $T_{3,n}$ admit an explicit expression [MMM]:

$$\mathcal{H}_{\text{Adj}}(T_{3,n}) = 2v^{2n} + D_{X_3} + q^{-4n}D_{Y_a} + q^{4n}D_{Y_b} - q^{-2n}D_{C_a} - q^{2n}D_{C_b}, \quad (11)$$

where

$$\begin{aligned} Y_a &= ([3], [3]), & Y_b &= ([1, 1, 1], [1, 1, 1]), & C_a &= ([2, 1], [3]) + ([3], [2, 1]), \\ C_b &= ([2, 1], [1, 1, 1]) + ([1, 1, 1], [2, 1]), & X_3 &= ([2, 1], [2, 1]) + ([3], [1, 1, 1]) + ([1, 1, 1], [3]), \end{aligned}$$

and

$$\begin{aligned} D_{Y_a} &= \frac{\{vq^5\}\{vq\}^2\{v\}^2\{v/q\}}{\{q^3\}^2\{q^2\}^2\{q\}^2}, & D_{Y_b} &= \frac{\{v/q^5\}\{v/q\}^2\{v\}^2\{vq\}}{\{q^3\}^2\{q^2\}^2\{q\}^2}, \\ D_{X_3} &= 2 \frac{\{vq^3\}\{vq\}\{vq^2\}\{v/q^2\}\{v/q\}\{v/q^3\}}{\{q^3\}^2\{q^2\}^2\{q\}^2} + \frac{\{vq^3\}\{vq\}^2\{v/q\}^2\{v/q^3\}}{\{q^3\}^2\{q\}^4}, \\ D_{C_b} &= \frac{2\{v\}^2\{\frac{v}{q^4}\}\{\frac{v}{q^2}\}\{vq\}\{vq^2\}}{\{q^3\}^2\{q^2\}\{q\}^3}; & D_{C_a} &= \frac{2\{v\}^2\{vq^4\}\{vq^2\}\{v/q\}\{v/q^2\}}{\{q^3\}^2\{q^2\}\{q\}^3}. \end{aligned}$$

Inserting these into Eq. (9) yields the HOMFLY-PT polynomial for reverse 2-cable torus knot $T_{3,n}$

$$P(C_2(T_{3,n}, -2n)) = \frac{1}{D_{[1]}} (1 + \mathcal{H}_{\text{Adj}}(T_{3,n})).$$

For clarity, we present selected examples in Tables 3 and 4, along with their corresponding geometric properties.

In accordance with Theorem 2.19, to evaluate the adjoint polynomial of torus knot $T(m, n)$, first one has to construct the m -plethystic expansion, and then find the quantum dimensions and the eigenvalues of the second Casimir operator. To illustrate, we explicitly present the 4-plethystic expansion as an example.

$(z \setminus v)$	-5	-3	-1	1	3	5	7
-1	-25	75	-85	45	-11	1	0
1	-100	350	-408	206	-44	2	2
3	-160	630	-757	349	-62	0	0
5	-130	585	-705	287	-37	0	0
7	-56	308	-363	121	-10	0	0
9	-12	93	-105	25	-1	0	0
11	-1	15	-16	2	0	0	0
13	0	1	-1	0	0	0	0

Table 3: HOMFLY-PT Polynomial(Panhandle polynomials) of the $C_2(T_{3,4}, -8)$ knot.

$(z \setminus v)$	-5	-3	-1	1	3	5	7	9	11	13
-1	-144	528	-760	536	-185	25	0	0	0	0
1	-1584	5920	-8234	5261	-1459	102	2	2	2	2
3	-7524	28596	-38772	22812	-5272	160	0	0	0	0
5	-20328	79028	-104710	57190	-11310	130	0	0	0	0
7	-34716	139820	-181104	91696	-15752	56	0	0	0	0
9	-39492	167820	-212434	98838	-14744	12	0	0	0	0
11	-30769	141165	-174526	73512	-9383	1	0	0	0	0
13	-16610	84645	-102103	38115	-4047	0	0	0	0	0
15	-6193	36349	-42715	13719	-1160	0	0	0	0	0
17	-1562	11090	-12672	3355	-211	0	0	0	0	0
19	-254	2346	-2601	531	-22	0	0	0	0	0
21	-24	327	-351	49	-1	0	0	0	0	0
23	-1	27	-28	2	0	0	0	0	0	0
25	0	1	-1	0	0	0	0	0	0	0

Table 4: HOMFLY-PT Polynomial(Panhandle polynomials) of the $C_2(T_{3,7}, -14)$ knot.

Example 2.24. The 4-plethystic expansion of the adjoint Schur function generating the Adams coefficients is

$$\begin{aligned} \widehat{\text{Ad}}_4 S_{\text{Adj}} = & 3 + S_{([1^4], [1^4])} - S_{([1^4], [2, 1, 1])} + S_{([1^4], [3, 1])} - S_{([1^4], [4])} - S_{([2, 1, 1], [1^4])} \\ & + S_{([2, 1, 1], [2, 1, 1])} - S_{([2, 1, 1], [3, 1])} + S_{([2, 1, 1], [4])} + S_{([3, 1], [1^4])} - S_{([3, 1], [2, 1, 1])} \\ & + S_{([3, 1], [3, 1])} - S_{([3, 1], [4])} - S_{([4], [1^4])} + S_{([4], [2, 1, 1])} - S_{([4], [3, 1])} + S_{([4], [4])}. \end{aligned}$$

The adjoint polynomials are

$$\mathcal{H}_{\text{Adj}}(T_{4,n}) = v^{2n} \left(3 + \sum_{\mu} \varepsilon_{\mu} D_{\mu}(v, q) q^{-\kappa_{\mu} n/4} \right),$$

where ε_{μ} is the sign factor coming from the Adams operation above. Explicit expressions for the quantum dimensions and the eigenvalues of the second Casimir operator in this formula are found in [BMi, Appendix A].

In the generic case, we need the following result.

Lemma 2.25 (Adjoint polynomials). **(i)** *The Adams operation $\widehat{\text{Ad}}_m$ applied to the character of the $SL(N)$ group in the adjoint representation gives rise to $m-1$ scalar terms at $N \geq m$:*

$$\widehat{\text{Ad}}_m S_{\text{Adj}} = (m-1) + \sum_{\mu} c_{\mu} S_{\mu}(v, q),$$

with some numeric coefficients c_{μ} .

(ii) The adjoint polynomials for $T_{m,n}$ take the following form:

$$\mathcal{H}_{\text{Adj}}(T_{m,n}) = v^{2n} \left((m-1) + \sum_{\mu} c_{\mu} D_{\mu}(q, v) q^{-\kappa_{\mu} n/m} \right). \quad (12)$$

Proof. First, one can use formula (10) and Theorem 2.19 and notice that if $R = \text{Adj}$, then $\kappa_{\text{Adj}} = 2N$ so that the common factor is indeed v^{2n} . Since the character of the $SL(N)$ group is equal to the Schur polynomial, we are interested in the scalar contribution into the Adams operation \widehat{Ad}_m , acting on the Schur function $S_{\text{Adj}}(x)$, the latter being a symmetric polynomial of variables x_i , $i = 1, \dots, N$. These variables are eigenvalues of the group element in the fundamental representation.

Now we notice that, in this case, the adjoint Schur function is equal to

$$S_{\text{Adj}} = S_{[2, 1^{N-2}]}(x) = (N-1) \mathfrak{m}_{[1^N]}(x) + \mathfrak{m}_{[2, 1^{N-2}]}(x), \quad (13)$$

where $\mathfrak{m}_R(x)$ is the monomial symmetric function. That is, since

$$\mathfrak{m}_{[1^N]}(x) = \prod_{i=1}^N x_i, \quad \mathfrak{m}_{[2, 1^{N-2}]}(x) = \sum_{\sigma} x_{i_1}^2 x_{i_2} x_{i_3} \dots x_{i_{N-1}} x_{i_N}^0,$$

where the sum runs over all possible permutations σ of the set $1, 2, \dots, N$, then¹

$$S_{[2, 1^{N-2}]}(x) = \prod_{k=1}^N x_k \sum_{i,j=1}^N \frac{x_i}{x_j} - \prod_{i=1}^N x_k. \quad (14)$$

Formula (13) reflects the fact that only two Kostka numbers $K_{[2, 1^{N-2}], \mu}$ (see definitions and properties in [Mac, §I.6]) are non-zero: the diagonal one (which is always equal to 1) and $K_{[2, 1^{N-2}], [1^N]} = N-1$.

The Adams operation \widehat{Ad}_m is associated with the m -plethysm of this formula corresponding to the substitution $x_i \rightarrow x_i^m$. The scalar contribution to \widehat{Ad}_m is associated with the Schur function $S_{\underbrace{[m, m, \dots, m]}_{N \text{ times}}} = \prod_{i=1}^N x_i^m$, since, in the $SL(N)$ case, $\prod_{i=1}^N x_i = 1$. Hence, we need to pick up from $\widehat{Ad}_m(S_{\text{Adj}})$ the term $S_{\underbrace{[m, m, \dots, m]}_{N \text{ times}}}$. To this end, we use “another scalar product” of [Mac, §VI.9], the Schur functions being orthogonal with this scalar product:

$$\begin{aligned} \langle f | g \rangle &= \frac{1}{N!} \oint \prod_{k=1}^N \frac{dx_k}{x_k} \prod_{i \neq j} \left(1 - \frac{x_i}{x_j} \right) f(x) g(x^{-1}) \\ \langle S_R, S_Q \rangle &= \delta_{RQ}. \end{aligned} \quad (15)$$

Here the integration contour encircles zero, and the measure is normalized so that $\oint \frac{dx}{x} = 1$. Then, the scalar contribution is

$$\left\langle \widehat{Ad}_m(S_{\text{Adj}}(x)) \mid S_{\underbrace{[m, m, \dots, m]}_{N \text{ times}}} \right\rangle = \left\langle S_{[2, 1^{N-2}]}(x^m) \mid \prod_{i=1}^N x_i^m \right\rangle.$$

Now, we use (14) and notice that

$$\left\langle \prod_{i=1}^N x_i^m \mid \prod_{i=1}^N x_i^m \right\rangle = \frac{1}{N!} \oint \prod_{k=1}^N \frac{dx_k}{x_k^{m+1}} \prod_{i \neq j} \left(1 - \frac{x_i}{x_j} \right) \prod_{n=1}^N x_n^m = 1$$

and that

¹Another way to obtain this formula is to notice that the adjoint representation is obtained from the expansion (see Remark 2.10) $[1] \otimes [\bar{1}] = \Phi \oplus \text{Adj}$, i.e. $\left(\sum_{i=1}^N x_i \right) \prod_{i=1}^N x_i \left(\sum_{i=1}^N x_i^{-1} \right) = \prod_{i=1}^N x_i + S_{\text{Adj}}$.

$$\begin{aligned}
\left\langle \prod_{k=1}^N x_k^p \sum_{i,j=1}^N \frac{x_i^m}{x_j^m} \mid \prod_{i=1}^N x_i^m \right\rangle &= \frac{1}{N!} \oint \prod_{k=1}^N \frac{dx_k}{x_k^{m+1}} \prod_{i \neq j} \left(1 - \frac{x_i}{x_j} \right) \sum_{n,m=1}^N \frac{x_n^m}{x_m^m} \prod_{s=1}^N x_s^m \\
&= \frac{1}{N!} \oint \prod_{k=1}^N \frac{dx_k}{x_k} \prod_{i \neq j} \left(1 - \frac{x_i}{x_j} \right) \sum_{n,m=1}^N \frac{x_n^m}{x_m^m} \\
&= \min(m, N).
\end{aligned}$$

Hence, we finally obtain from (14) that

$$\left\langle S_{[2,1^{N-2}]}(x^m) \mid \underbrace{S_{[m,m,\dots,m]}}_{N \text{ times}} \right\rangle = \min(m, N) - 1,$$

which is equal to $m - 1$ at large enough N . This completes the proof. \square

Now we make a claim about the generic structure of the sum in Lemma 2.25.

Lemma 2.26 (Structure of sums). *Consider the Young diagrams μ entering the sum in Lemma 2.25. Then the following hold:*

- (i) *The quantum dimensions $D_\mu(q, v)$ are all Laurent polynomials of v of maximal degree $2m$ and minimal degree $-2m$.*
- (ii) *$\kappa_\mu - 2mN$ does not depend on N .*

Proof. The diagrams μ are all associated with composite representations [Ko]. Moreover, since the representations belong to the m -th power of the adjoint representation, $([1], [1])$, all of them have the form (R, P) with $|R| = |P| := \mathfrak{p} \leq m$. The quantum dimension of the composite representation is given by [MM, Formula (28)], which can be rewritten in the form

$$D_{(R,P)}(q, v) = D_R(q, vq^{-l_p}) D_P(q, vq^{-l_R}) \prod_{i=1}^{l_R} \prod_{j=1}^{l_p} \frac{[N + R_i + P_j + 1 - i - j]_q}{[N - i - j + 1]_q}, \quad (16)$$

where l_R denotes the number of lines in the Young diagram R . Since the quantum dimension can not have poles at integer N , the factors in the denominator are canceled with some factors in the numerator. Taking into account Definition 2.14, it follows directly that the total number of factors containing $v = q^N$, all of them being of the form $\{vq^\alpha\}$ with some α , is $|P| + |R| = 2\mathfrak{p}$. Hence, the quantum dimension of the representation (R, P) is a Laurent polynomials of $v = q^N$ of maximal degree $|P| + |R| = 2\mathfrak{p}$ and of minimal degree $-|P| - |R| = -2\mathfrak{p}$.

One can also evaluate the eigenvalue of the second Casimir operator in the composite representation (R, P) with $|R| = |P| = \mathfrak{p}$. It is given by

$$\kappa_{(R,P)} = 2N\mathfrak{p} + \kappa_R - \kappa_{P^T}. \quad (17)$$

Now note that, in accordance with this formula and Lemma 2.25 (ii), the coefficient in front of the quantum dimension D_μ enters the HOMFLY-PT polynomial with degree of v equal to $2n(m - \mathfrak{p})/m$. This degree is a non-negative even number, and m and n are co-prime for knots, hence we have $\mathfrak{p} = m$, and

$$\kappa_{(R,P)} - 2Nm = \kappa_R - \kappa_{P^T}.$$

This proves the Lemma. \square

2.3 Proof of the Panhandle theorem for torus knots

From Lemmas 2.25 and 2.26, one can immediately prove the main theorem.

Proof of Theorem 1.1. Indeed, in accordance with Lemma 2.25 and Lemma 2.26(ii), the term depending on n can be presented in the form

$$(m-1)zv \frac{v^{2n} - v^{2m}}{v^2 - 1}.$$

Now, since the numerator vanishes at $v = \pm 1$ and $P(C_2(T_{m,n}, t))$ is a polynomial in v , such is the difference

$$P(C_2(T_{m,n}, t)) - (m-1)zv \frac{v^{2n} - v^{2m}}{v^2 - 1}.$$

Now, from Lemma 2.26(i) it follows that this difference divided by $D_{[1]}$, call it X , is $[1-2m; 2m-1]_v$, except that we need to clarify why in (1)

$$\min \deg_v X = 1-2m, \quad \max \deg_v X = 2m-1 \quad (18)$$

instead of $\min \deg_v X \geq 1-2m$, $\max \deg_v X \leq 2m-1$. That is, we show that no cancellations occur in the μ -summation of (12) in the highest or lowest degree v -term. (This argument appears in modified form in [St1], but is repeated here for completeness.)

We consider only $X = [P(C_2(T_{m,n}, t))]_{z^{-1}}$, and prove (18) this way. It is well known from skein theory [LM] that

$$[P(C_2(K, t))]_{z^{-1}} = v^{2t} (v^{-1} - v) ([P(K)]_{z^0})^2. \quad (19)$$

Notice that for $K = T_{m,n}$ we have

$$\min \deg_v P(K) = (m-1)(n-1) = 2g(K), \quad (20)$$

with $g(K)$ the genus. Therefore, to prove (18), it is enough to prove the two claims

$$[P(K)]_{z^0 v^{(n\pm 1)(m-1)}} \neq 0. \quad (21)$$

For this, we use skein theory, and Nakamura's observation [Na]. Assume that $\beta \in B_r$ is a positive braid word (in the Artin generators σ_j). Then for $\beta_{[i]} = \beta \sigma_j^i$ and $j = 1, \dots, r-1$ fixed, and any $x, s \in \mathbb{Z}$, we have for $L_i = \hat{\beta}_{[i]}$, and $L = L_0$,

$$|[P(L_2)]_{z^x v^{s+2}}| = |[P(L_1)]_{z^{x-1} v^{s+1}}| + |[P(L)]_{z^x v^s}|. \quad (22)$$

We write by $\chi(L)$ the maximal Euler characteristic of a Seifert surface of a link L , and by $l(L)$ be the number of components of L . Now in (22) we set $x = 1 - l(L)$, $s = 1 - \chi(L)$, and $r = m$.

Let us write $\beta_1 \succ \beta_2$ if $\beta_1 \in \{\alpha, \alpha \sigma_j\}$ and $\beta_2 = \alpha \sigma_j^2$ for a positive braid word α . We further allow to permute letters cyclically in the β_i . Transitively expand this relation \succ to become a partial order.

Assume that β is a positive braid so that there is a sequence $(\beta = \beta_k, \beta_{k-1}, \dots, \beta_0)$ with $\hat{\beta}_0 = T_{m,n}$, and $\beta_{i-1} \succ \beta_i$. Then for $L = \hat{\beta}$ and $l(L)$ components, and $y \geq 0$,

$$|[P(T_{m,n})]_{z^0 v^{(m-1)(n-1)+y}}| \geq |[P(L)]_{z^{1-l(L)} v^{1-\chi(L)+y}}|. \quad (23)$$

It follows from (22). Note that when $l(L_1) = l(L) - 1$ (and not $l(L) + 1$), then the first term on the right of (22) is zero.

We start with $\beta_0 = \tau_{m,n} := (\sigma_1 \dots \sigma_{m-1})^n$. This braid contains the center twist $\Delta_m^2 = (\sigma_1 \dots \sigma_{m-1})^m$, and it is easy to see that for every positive words α, γ , we have $\Delta_m^2 \alpha \gamma \succ \Delta_m^2 \gamma$. This is because one can write $\Delta_m^2 = \delta \sigma_j$ with a positive word δ for every $j = 1, \dots, m-1$. Thus

$$\tau_{m,n} \succ \tau_{m,m} = \Delta_m^2. \quad (24)$$

Because of (23), this means that for (21) it is enough to check that the right-hand side of (23) is non-zero for L being the closure of $\beta_k = \Delta_m^2$, and $y = 0, y = 2(m-1)$. But this L is an m -component link of m unknotted components. We have

$$[P(L)]_{z^{1-m}} = v^{1-\chi(L)} (v^{-1} - v)^{m-1}$$

by the known generalization of (19). Therefore (21) follows. \square

2.4 Extension to torus links

In the case of links, the Rosso-Jones formula ([LZ, Theorem 5.1][RJ, Theorem 8]) reads:

Theorem 2.27. *Consider L be the torus link with l components, $T(m, n)$, where m/l and n/l are relatively prime integers. Let $R \vdash s$ be a partition. Then, the reduced colored HOMFLY-PT polynomial of L with all components colored by R in the vertical framing is given by:*

$$\mathcal{H}_R(L) = q^{n\kappa_R} \cdot \sum_{\mu \vdash sm} c_\mu^R \cdot q^{-n\kappa_\mu/m} \cdot D_\mu(q, v),$$

where c_μ^R are the integers determined by

$$\left(\widehat{Ad}_{m/l} S_R(x_1, x_2, \dots) \right)^l = \left(S_R(x_1^{m/l}, x_2^{m/l}, \dots) \right)^l = \sum_{\mu \vdash ms} c_\mu^R \cdot s_\mu(x_1, x_2, \dots).$$

Remark 2.28. This theorem is originally formulated in [LZ][RJ] for the link with components colored with l generally different partitions. However, we do not need this more general case here.

Examples of torus links $T(2, 2n)$ and $T(3, 3n)$ can be found in [MMM]. Now, let us make an inspection of the generic link. Of the two essential Lemmas 2.25 and 2.26, the analogue of the first, for links, reads:

Lemma 2.29 (Adjoint polynomials). **(i)** *The Adams operation \widehat{Ad}_m applied to the character of the $SL(N)$ group in the adjoint representation to the power l gives rise to $\zeta_{m,l}$ scalar terms at $N \geq m$ with*

$$\zeta_{m,l} := \sum_{k=0}^l (-1)^{l+k} \frac{l!}{(l-k)!} \left(\frac{m}{l} \right)^k \quad (25)$$

so that $\zeta_{m,l} \neq 0$ unless $m = l = 1$.

(ii) *The adjoint polynomials for $T(m, n)$ take the following form:*

$$\mathcal{H}_{\text{Adj}}(T(m, n)) = v^{2n} \left(\zeta_{m,l} + \sum_{\mu} c_{\mu}^{\text{Adj}} D_{\mu}(q, v) q^{-\kappa_{\mu} n/m} \right). \quad (26)$$

Proof. First of all, using formula (10) and Theorem 2.27 and noticing that, for $R = \text{Adj}$, $\kappa_{\text{Adj}} = 2N$, one states that the common factor is v^{2n} . In order to evaluate $\zeta_{m,l}$, we again use that the adjoint Schur function is given by (13), and we are interested in the scalar contribution into degree l of the Adams operation $\left(\widehat{Ad}_{m/l} S_{\lambda}(x_1, x_2, \dots) \right)^l$ as in the Rosso-Jones theorem 2.27.

The scalar contribution to the Adams operation is associated with the Schur function $S_{\underbrace{[m, m, \dots, m]}_{N \text{ times}}} = \prod_{i=1}^N x_i^m$, since, in the $SL(N)$ case, $\prod_{i=1}^N x_i = 1$. Hence, we need to pick up from $\left(\widehat{Ad}_{m/l} S_{\lambda}(x_1, x_2, \dots) \right)^l$ the term $S_{\underbrace{[m, m, \dots, m]}_{N \text{ times}}}$.

To this end, we again use “another scalar product” (15). Then, the scalar contribution is

$$\left\langle \left(\widehat{Ad}_{m/l}(S_{\text{Adj}}(x)) \right)^l \middle| \underbrace{S_{[m, m, \dots, m]}}_{N \text{ times}} \right\rangle = \left\langle \left(S_{[2, 1^{N-2}]}(x^{m/l}) \right)^l \middle| \prod_{i=1}^N x_i^m \right\rangle.$$

Now, we use (14),

$$\left(S_{[2, 1^{N-2}]}(x^{m/l}) \right)^l = \prod_{j=1}^N x_j^m \left(\sum_{i,j=1}^N \frac{x_i^{m/l}}{x_j^{m/l}} - 1 \right)^l = \prod_{j=1}^N x_j^m \sum_{k=0}^l (-1)^{l+k} \binom{l}{k} \left(\sum_{i,j=1}^N \frac{x_i^{m/l}}{x_j^{m/l}} \right)^k \quad (27)$$

and notice that, at $N \geq pk/l$,

$$\left\langle \prod_{j=1}^N x_j^m \left(\sum_{i,j=1}^N \frac{x_i^{m/l}}{x_j^{m/l}} \right)^k \middle| \prod_{i=1}^N x_i^m \right\rangle = \frac{1}{N!} \oint \prod_{j=1}^N \frac{dx_j}{x_j^{m+1}} \prod_{i \neq j} \left(1 - \frac{x_i}{x_j} \right) \left(\sum_{i,j=1}^N \frac{x_i^{m/l}}{x_j^{m/l}} \right)^k \prod_{s=1}^N x_s^m = k! \left(\frac{m}{l} \right)^k.$$

This formula, along with (27), implies that, at $N \geq m$,

$$\begin{aligned} \left\langle \left(S_{[2,1^{N-2}]}(x^{m/l}) \right)^l \middle| \underbrace{S[m,m,\dots,m]}_{N \text{ times}} \right\rangle &= \sum_{k=0}^l (-1)^{l+k} \binom{l}{k} \left\langle \prod_{j=1}^N x_j^m \left(\sum_{i,j=1}^N \frac{x_i^{m/l}}{x_j^{m/l}} \right)^k \middle| \prod_{i=1}^N x_i^m \right\rangle \\ &= \sum_{k=0}^l (-1)^{l+k} \frac{l!}{(l-k)!} \left(\frac{m}{l} \right)^k, \end{aligned}$$

which exactly matches $\zeta_{m,l}$ in (25). This completes the proof. \square

Remark 2.30 (Consistency checks). Formula (25) is, indeed, equal to $m-1$ for knots, i.e., at $l=1$. Moreover, it is equal to 1 at $m=2, l=2$ and is equal to 2 at $m=3, l=3$, which perfectly matches the answers in [MMM].

Lemma 2.31 (Adjoint polynomials). *Let $X = [[\underline{M}; M]]_v$ denote a polynomial such that*

$$\min \deg_v X \geq \underline{M} \quad \text{and} \quad \max \deg_v X \leq M. \quad (28)$$

(i) *The adjoint polynomial (26) can be presented in the form*

$$\mathcal{H}_{\text{Adj}}(T(m,n)) = v^{2n} \zeta_{m,l} + \sum_{k=1}^l [[-2mk/l; 2mk/l]]_v v^{2n(l-k)/l}. \quad (29)$$

(ii) *This adjoint polynomial normalized to unknot is*

$$\frac{1}{\mathcal{H}_{[1]}(U)} \mathcal{H}_{\text{Adj}}(T(m,n)) = z \frac{P(v)}{\{v\}} + \sum_{k=1}^l [[-2mk/l+1; 2mk/l-1]]_v v^{2n(l-k)/l} \quad (30)$$

where $P(v)$ is a polynomial of v only.

Proof. First, let us notice that, similarly to the knot case, the diagrams μ are composite representations having form (R, P) with $|R| = |P| = \mathfrak{p} \leq m$. In the link case, in accordance with Lemma 2.29 and formula (17), the diagram μ enters the HOMFLY-PT polynomial with degree of v equal to $2n(m-\mathfrak{p})/m$, which is a non-negative even integer. Since, in the case of l -component link, both n and m are divided by l , one concludes that any $\mathfrak{p} = mk/l, k = 1, \dots, l$ may appear in (26). Now using Lemma 2.26(i), one concludes that formula (26) takes the form (29). This proves part (i).

By a direct analysis of formula (16), one establishes that the quantum dimension of composite representation (R, P) behaves at the vicinity of $v^2 = 1$ as

$$D_{(R,P)}(q, v) \approx \sum_{k=0} d_k(q) \{v\}^k \quad (31)$$

and the coefficient d_0 does not depend on q . This proves (ii). \square

Another point that has to be corrected in the link case is Definition 2.10. Note that for torus links the vertical framing (3) must be modified to

$$t_v = \left(\underbrace{\left(1 - \frac{m}{l} \right) \frac{n}{l}, \dots, \left(1 - \frac{m}{l} \right) \frac{n}{l}}_{l \text{ times}} \right). \quad (32)$$

Definition 2.32 (HOMFLY-PT polynomial for *reverse 2-cable link*). Let L be a link with l components, and let $\mathcal{H}_{\{R_\alpha\}}(L)$ denotes the colored HOMFLY-PT polynomial of L colored by a set of Young tableaux representations $R_\alpha, \alpha = 1, \dots, l$ of the group $U_q(\mathfrak{sl}_N)$. Given

$$R^{(\alpha)} \otimes \bar{R}^{(\alpha)} = \bigoplus_i Q_i^{(\alpha)},$$

with each $Q_i^\alpha \in \text{Rep}(U_q(\mathfrak{sl}_N))$, the colored HOMFLY-PT polynomial (un-normalized) of the *reverse 2-cable link* is given by

$$\mathcal{H}_{\{R_1, \dots, R_l\}}(C_2(L, t_v)) := \sum_{i_1, \dots, i_l} \mathcal{H}_{Q_{i_1}^{(1)}, \dots, Q_{i_l}^{(l)}}(L).$$

The HOMFLY-PT polynomial(normalized) of the reverse 2-cable link $T(m, n)$ with l components is

$$P(C_2(T(m, n), t_v)) = \frac{1}{\mathcal{H}_{[1]}(U)} \sum_{k=0}^l \binom{l}{k} \mathcal{H}_{\text{Adj}}(T(mk/l, nk/l)), \quad (33)$$

where we put $\mathcal{H}_{\text{Adj}}(T(0, 0)) = 1$.

Example 2.33 (2-cable links $T(2, n)$ and $T(3, n)$). The fundamental normalized HOMFLY-PT polynomial of the reverse 2-cable link $T(2, n)$:

$$P(C_2(T(2, n), t_v)) = \frac{1}{\mathcal{H}_{[1]}(U)} \left(1 + 2 \underbrace{\mathcal{H}_{\text{Adj}}(T(1, n/2))}_{D_{\text{Adj}}} + \mathcal{H}_{\text{Adj}}(T(2, n)) \right). \quad (34)$$

Similarly, the reverse 2-cable link $T(3, n)$ is

$$P(C_2(T(3, n), t_v)) = \frac{1}{\mathcal{H}_{[1]}(U)} \left(1 + 3D_{\text{Adj}} + 3\mathcal{H}_{\text{Adj}}(T(2, 2n/3)) + \mathcal{H}_{\text{Adj}}(T(3, n)) \right). \quad (35)$$

The following generalizes Theorem 1.1 to the link case. In analogy to (1) and (28), say that $[\underline{M}; M]_v$ stands for a polynomial X with $\min \deg_v X = \underline{M}$ and $\max \deg_v X \leq M$.

Theorem 2.34 (Panhandle for links). *The HOMFLY-PT polynomial for the reverse 2-cable l -component torus link $C_2(T_{m, n}, t_v)$ has the form*

$$P(C_2(T_{m, n}, t_v)) = \left[1 - 2m; 2n \frac{l-1}{l} + \frac{2m}{l} - 1 \right]_v + \underbrace{\zeta_{m, l} z v \frac{v^{2n} - v^{2m}}{v^2 - 1}}_{\text{panhandle}}. \quad (36)$$

Hence, the length of the link panhandle is equal to $2(n - m)/l$.

Proof. This follows from Lemma 2.31(i) and formula (33). In particular, the panhandle contributions to (36) from $\mathcal{H}_{\text{Adj}}(T(mk/l, nk/l))$ give rise to $v^{2nk/l}$ terms, which are parts of the polynomial $[1 - 2m; 2n \frac{l-1}{l} + 2m/l - 1]_v$ at $k \neq l$. It remains to prove that the polynomial $[1 - 2m; 2n \frac{l-1}{l} + 2m/l - 1]_v$ in the Theorem is exactly this, and not just $[[1 - 2m; 2n \frac{l-1}{l} + 2m/l - 1]]_v$, i.e., that the coefficient in front of v^{1-2m} does not vanish. To this end, we use the proof of (18), which holds but will not be explicitly repeated here. \square

Remark 2.35 (Consistency check). This Theorem reduces to Theorem 1.1 at $l = 1$. Note also that, when $m = n$, we still obtain $\max \deg_v P(C_2(T_{m, n}, t_v)) = 2n - 1$ because the argument behind (18) remains valid.

Example 2.36 (Link $T(3, 12)$). As an illustration of the Theorem, the coefficients for $T(3, 12)$ are given in Table 5. One can see that, starting with z^{23} , there is only the scalar contribution (yellow boxes); at z^{17} , there also emerges the contribution from $\mu = \text{Adj}$ with $\mathfrak{p} = 1$ (green boxes); starting with z^{11} , there are contributions with $\mathfrak{p} = 2$ (blue boxes), and, at last, starting with z^5 , those with $\mathfrak{p} = 3$. In fact, $\mathcal{H}_{\text{Adj}}(T(2, 8))$ due to formula (35) also contributes to this table: starting with z^{15} , there is its panhandle contribution², and contributions of $\mathfrak{p} = 1$ and $\mathfrak{p} = 2$ first emerge at z^9 and z^3 accordingly. The sum of numbers at every line of the table is equal to zero, which is the vanishing of the Conway polynomial due to the link bounding a disconnected Seifert surface.

²For instance, the term $z v^{15}$ comes from the sum of $-9zv^{15}$ contribution from $\mu = \text{Adj}$ of $\mathcal{H}_{\text{Adj}}(T(3, 12))$ in (26) — $c_{\text{Adj}}^{\text{Adj}} = 9$ in this case — of $2zv^{15}$ panhandle contribution from $\mathcal{H}_{\text{Adj}}(T(3, 12))$, and of $3zv^{15}$ panhandle contribution from $\mathcal{H}_{\text{Adj}}(T(2, 8))$, which totally gives $-4zv^{15}$.

$(z \setminus v)$	-5	-3	-1	1	3	5	7	9	11	13	15	17	19	21	23
-5	-11	-11	-10	26	5	1	0	0	0	0	0	0	0	0	0
-3	-2138	-3123	-475	3789	1911	30	18	-18	6	0	0	0	0	0	0
-1	-73146	-112956	-9402	124628	70234	522	330	-282	72	0	-9	9	0	0	0
1	-996684	-1584078	-95046	1681752	987298	5984	2126	-1624	272	-4	-4	2	2	2	2
3	-7184691	-11634737	-592970	12111874	7254903	43737	5676	-4164	372	0	0	0	0	0	0
5	-31609050	-51945059	-2466115	53420915	32403009	194098	7770	-5790	222	0	0	0	0	0	0
7	-92427173	-153901035	-7147177	156866451	96049439	558115	6012	-4692	60	0	0	0	0	0	0
9	-189895362	-320221087	-14912425	323970681	199954829	1102890	2730	-2262	6	0	0	0	0	0	0
11	-284749628	-486266654	-22982519	488654927	303785858	1557932	720	-636	0	0	0	0	0	0	0
13	-319999214	-553472921	-26692421	552641876	345909242	1613432	102	-96	0	0	0	0	0	0	0
15	-274472117	-480911809	-23716007	477208635	300647119	1244179	6	-6	0	0	0	0	0	0	0
17	-181826796	-322794482	-16287176	318353438	201834960	720056	0	0	0	0	0	0	0	0	0
19	-93628147	-168439053	-8695805	165120651	105329345	313009	0	0	0	0	0	0	0	0	0
21	-37521836	-68412618	-3613274	66665888	42780334	101506	0	0	0	0	0	0	0	0	0
23	-11653501	-21532555	-1163599	20862369	13465831	24155	0	0	0	0	0	0	0	0	0
25	-2774868	-5197330	-287336	5005906	3249538	4090	0	0	0	0	0	0	0	0	0
27	-496702	-942884	-53355	903021	589454	466	0	0	0	0	0	0	0	0	0
29	-64640	-124350	-7206	118434	77730	32	0	0	0	0	0	0	0	0	0
31	-5771	-11249	-668	10656	7031	1	0	0	0	0	0	0	0	0	0
33	-316	-624	-38	588	390	1	0	0	0	0	0	0	0	0	0
35	-8	-16	-1	15	10	0	0	0	0	0	0	0	0	0	0

Table 5: HOMFLY-PT Polynomial of $C_2(T_{3,12}, (0,0,0))$.

Remark 2.37 (Large n behavior). In fact, at large enough n , contributions into $C_2(T_{m,n}, t_v)$ are well-separated in degrees of v , excluding the one linear in z , because of the panhandle contributions. This follows from Lemma 2.31(ii).

Example 2.38 ($n = 42$). For instance, for $C_2(T_{3,42}, (0,0,0))$, one can observe that

$$\begin{aligned}
 C_2(T_{3,42}, (0,0,0)) &= z^{-5}([-5,5]_v + [-3,3]_v v^{28}) + \\
 &+ z^{-3}([-5,5]_v + [-3,3]_v v^{28}) + \\
 &+ z^{-1}([-5,5]_v + [-3,3]_v v^{28} + 9(v^2 - 1)v^{55}) + \\
 &+ z\left([-5,5]_v + [-3,3]_v v^{28} - 6v\frac{v^{56} - v^{28}}{v^2 - 1} + 2v\frac{v^{84} - 1}{v^2 - 1}\right) + \\
 &+ z^3([-5,5]_v + [-3,3]_v v^{28}) + \\
 &\dots \\
 &+ z^{35}([-5,5]_v + [-3,3]_v v^{28}).
 \end{aligned} \tag{37}$$

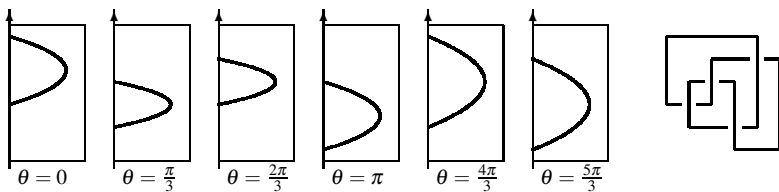
The polynomials $[-5,5]_v$ and $[-3,3]_v$ in this formula are definitely distinct at distinct degrees of z . We do not display the table for this case because of its large size.

3 Geometric properties

In the following subsections, we outline the geometric consequences of Theorem 1.1. However, we do not like to go into details, since they require the introduction of a series of different tools. For this, see the sequel of papers [JLS1][JLS2][St1], with only the relevant part of these papers is summarized here.

3.1 Arc index and Thurston-Bennequin invariant

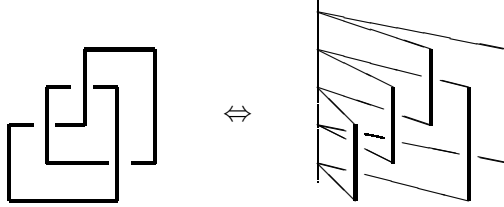
An *arc presentation* of a knot or a link L is an ambient isotopic image of L contained in the union of finitely many half-planes, called *pages*, with a common boundary line in such a way that each half plane contains a properly embedded single arc.



The minimal number of pages among all arc presentations of a link L is called the *arc index* of L and is denoted by $a(L)$. See [MB].

A *grid diagram* is a knot diagram which is composed of finitely many horizontal edges and the same number of vertical edges, such that vertical edges always cross over horizontal edges. It is not hard to see that every knot admits a grid diagram.

The figure below explains that arc presentations and grid diagrams correspond one-to-one.



Let $\iota(D)$ be the *size* of a grid diagram, the number of horizontal (or equivalently, vertical) segments. Thus

$$a(K) = \min \{ \iota(D) : D \text{ is a grid diagram of } K \}.$$

We say D is a *minimal grid diagram* of K if $\iota(D) = a(K)$.

There is a further correspondence: when a grid diagram of K is rotated by $\pi/4$, then it can be seen as a *Legendrian front diagram* of a Legendrian embedding of K . See [LN][Ta1][FT].

There is an invariant of Legendrian isotopy, called *Thurston-Bennequin invariant/number*. We define it here equivalently in terms of a grid diagram.

Definition 3.1. The *Thurston-Bennequin invariant* of a grid diagram D , written $TB(D)$, is defined as

$$TB(D) = -Z(D) + w(D), \quad (38)$$

where $w(D)$ is the writhe of D (taken as a planar diagram of K) and $Z(D)$ the number of NW- or SE-corners of D .

Definition 3.2. The *maximal Thurston-Bennequin invariant* of a knot K , written $TB(K)$ is

$$TB(K) = \max \{ TB(D) \mid D \text{ is a grid diagram of } K \}.$$

3.2 Braid index and braided surfaces

Let $b(K)$ be the braid index of K , the minimal number of strings of a braid representative of K . By the MFW inequalities [Mo][FW], the writhe w of an r -string braid representative of L satisfies

$$w + r - 1 \geq \max \deg_v P(L) \geq \min \deg_v P(L) \geq w - r + 1, \quad (39)$$

so that

$$MFW(L) := \frac{1}{2} \text{span}_v P(L) + 1 \leq b(L), \quad (40)$$

where the left-hand side is the *MFW bound* for the braid index $b(L)$. If $MFW(L) = b(L)$, we say that L is *MFW-sharp*.

The Artin generators σ_i (see (4)) are generalized to the *band generators* [BKL]

$$\sigma_{i,j} = \sigma_i \dots \sigma_{j-2} \sigma_{j-1} \sigma_{j-2}^{-1} \dots \sigma_i^{-1}, \quad (41)$$

so that $\sigma_i = \sigma_{i,i+1}$.

A representation of a braid β , and its closure link $L = \hat{\beta}$, as a word in $\sigma_{i,j}^{\pm 1}$ is called a *band representation*. A band representation of β spans naturally a Seifert surface S of the link L : one glues disks into the strands, and connects them by half-twisted bands along the $\sigma_{i,j}$. The resulting surface is called *braided Seifert surface* of L . In

fact, a result of Rudolph [Ru2] (later rediscovered independently by M. Hirasawa) says that any Seifert surface is of this form.

A minimal genus braided Seifert surface S is called a *Bennequin surface* (see [BMe]). If S is realizable as Bennequin surface on $b(L)$ strings, then S is called a *minimal string Bennequin surface* of L . By Bennequin and Birman-Menasco [BMe], a 3-braid link L has a minimal string Bennequin surface. However, by [HS], we know that this is not true for 4-braid knots already. For more work on minimal string Bennequin surfaces, see [St2].

3.3 Quasipositivity and strong quasipositivity

A link is called *quasipositive* if it is the closure of a braid β of the form

$$\beta = \prod_{k=1}^l w_k \sigma_{i_k} w_k^{-1}, \quad (42)$$

where w_k is any braid word and σ_{i_k} is a (positive) standard Artin generator of the braid group (see [BO]). If the words $w_k \sigma_{i_k} w_k^{-1}$ are of the form σ_{i_k, j_k} in (41), so that

$$\beta = \prod_{k=1}^l \sigma_{i_k, j_k}, \quad (43)$$

then they can be regarded as embedded bands. Links which arise this way, i.e., such with *positive band presentations*, are called *strongly quasipositive links*. An overview of this topic can be found in [Ru1].

Question 3.3. (Rudolph; see [St3, Remark 8.3.3]) If L is strongly quasipositive, does L have a strongly quasipositive braid representative on $b(L)$ strands?

In the course of routine tabulation, the fourth author has confirmed this for strongly quasipositive prime knots up to 16 crossings, for example.

We write again $\chi(L)$ for the maximal Euler characteristic of L , as in the proof of Theorem 1.1 in §2.3, and $w(\beta)$ is the writhe/exponent sum of the braid β .

Theorem 3.4 (Bennequin [Be]). *For $\hat{\beta} = L$, for $\beta \in B_r$, one has*

$$-\chi(L) \geq w(\beta) - r.$$

Thus, Bennequin's work implies that any *strongly quasipositive Seifert surface*, a braided Seifert surface with only positive bands, is a Bennequin surface: if a link L has a strongly quasipositive Seifert surface S on r strands with ι bands, then $\chi(L) = \chi(S) = r - \iota$.

There is a similar version of this inequality for $\chi_4(L)$, the *(smooth) slice Euler characteristic* of L ,

$$-\chi_4(L) \geq w(\beta) - r. \quad (44)$$

This is sometimes called the *slice Bennequin inequality*.

Corollary 3.5. *Every strongly quasipositive surface is a Bennequin surface.*

Baker-Motegi asked if every minimal genus surface of a strongly quasipositive link is strongly quasipositive. (See §4.2.4.) This is an open question. For some work on this question, see [St2].

We also note that the aforementioned examples with Hirasawa [HS] are not strongly quasipositive. Thus one cannot use their Bennequin surfaces to address Question 3.3.

Definition 3.6. A link L is *Bennequin-sharp* if

$$-\chi(L) = \max \{ w(\hat{\beta}) - r \mid \hat{\beta} = L, \beta \in B_r \}.$$

Similarly, it is *slice Bennequin-sharp* if the inequality (44) can be made into an equality for proper β .

Corollary 3.7. *If L is strongly quasipositive, then L is Bennequin-sharp.*

Problem 3.8 (Bennequin sharpness problem; see, e.g., [FLL, St2]). A link L is strongly quasipositive if and only if L is Bennequin-sharp.

Returning to $C_2(K, t)$ (recall Definition 2.10), set

$$\lambda(K) := \min\{ t \mid C_2(K, t) \text{ is strongly quasipositive} \}.$$

The following was known to Rudolph, but its reproof in [JLS1] yields a fundamental insight into the new applications.

Theorem 3.9 (Rudolph; see [JLS1]). *If $K \neq U$ is non-trivial, then we have $\lambda(K) = -TB(K)$. Furthermore, $C_2(K, t)$ is strongly quasipositive if and only if $t \geq \lambda(K)$.*

This relationship originates from a construction, noted by Rudolph (see [Ru3, Fig. 1]) and later by Nutt (cf. [Nu, Theorem 3.1]), which will be referred to as *grid-band construction*. See further [JLS1][JLS2]. Note that for the unknot $\lambda(U) = 0$ but $-TB(U) = 1$. We again prefer to use the symbol $\lambda(K)$ instead of $TB(K)$ in the sequel. (To obtain the statements about the maximal Thurston-Bennequin invariant, reverse signs. The unknot can always be handled *ad hoc*.)

Definition 3.10. We write $W_{\pm}(K, t)$ for the *Whitehead double* of a knot K with framing t and positive/negative clasp.

Rudolph's work also implies the following.

Theorem 3.11 (see [JLS2]). *We have that $W_+(K, t)$ is strongly quasipositive if and only if $t \geq \lambda(K)$. And $W_-(K, t)$ is never strongly quasipositive.*

What is discussed in [St1] is the quasipositivity of these links. In particular, we know there with S. Orevkov that it is *not* always equivalent to their strong quasipositivity. We should emphasize here the connection between $\lambda(K)$ and $a(K)$. When D is a grid diagram of a knot K , then one can regard the *mirror image* $!D$ as grid diagram of the mirrored knot $!K$, by changing all crossings and rotating by $\pm\pi/2$. With (38), set

$$\lambda(D) = -TB(D) = Z(D) - w(D).$$

It is straightforward to observe

$$\lambda(D) + \lambda(!D) = \iota(D).$$

Theorem 3.12 (Dynnikov-Prasolov [DP]). *If D is a minimal grid diagram of $K (\neq U)$, then $\lambda(D) = \lambda(K)$.*

This yields the important relationship (that had been conjectured previously)

$$\lambda(K) + \lambda(!K) = a(K). \tag{45}$$

3.4 Properties of torus knots

Now we start relating the previous setting to Theorem 1.1. We defined two invariants [JLS2], which are slightly rephrased here as follows.

Definition 3.13 ([JLS2]). Let K be a knot. Assume $t \in \mathbb{Z}$ is chosen so that

$$\min \deg_z P(C_2(K, t)) = 1 - 2m < 0, \quad \max \deg_z P(C_2(K, t)) = 2n - 1 > 0, \tag{46}$$

for positive integers m, n . Then set

$$\ell(K) := 1 + \frac{1}{2} \operatorname{span}_v P(C_2(K, t)) = m + n \tag{47}$$

and

$$\theta(K) := t + m. \tag{48}$$

Observe that since $C_2(K, t)$ is a 2-component link, $\min \deg_z P(C_2(K, t))$ and $\max \deg_z P(C_2(K, t))$ are always odd. It is also easy to see from (19) that for every K there is a t with (46).

We recall that t can be extracted from $P(C_2(K, t))$, and in fact in two independent ways. One is (19). But an even simpler way is

$$t = [P(1, z)]_z,$$

using that the Conway polynomial $\nabla(z) = P(1, z)$ contains the linking number. (This was used in the much more complicated definition of $\theta(K)$ than (48), given in [JLS2], which does not assume (46).) Note further the property

$$\theta(K) + \theta(!K) = \ell(K),$$

in analogy to (45).

Theorem 3.14 ([JLS2]). *For every non-trivial knot K ,*

$$\ell(K) \leq a(K) \quad \text{and} \quad \theta(K) \leq \lambda(K).$$

Theorem 3.14 with Theorem 1.1 implies a result of Etnyre-Honda about the arc index of the torus knot [EH],

$$a(T_{m,n}) = m + n. \tag{49}$$

(As noted in [St1], this conclusion is not possible from [MB] when p is odd.) Theorem 3.14 also yields Etnyre-Honda's other result

$$\lambda(T_{m,n}) = -mn + m + n, \quad \lambda(!T_{m,n}) = mn. \tag{50}$$

(We continue using ‘!’ for ‘mirror image’.)

Notice, also for later reference, that $T_{m,n}$ has a grid diagram D of size $\iota(D) = m + n$, which is the obvious generalization of the shown here for $m = 3$ and $n = 5$.



We will refer to this diagram and its planar mirror image for $!T_{m,n}$ as the *standard grid diagram*.

Note that the reverse inequalities needed for (49) and (50), are directly realized by looking at this standard grid diagram D of $T_{m,n}$ and reading off its Thurston-Bennequin invariant $TB(D)$ in (38). Note also that $\lambda(T_{m,n}) = 1 - 2g(T_{m,n})$ with (20), as follows alternatively from [Ta2], since $T_{m,n}$ is a positive knot.

The property (49) exhibits $T_{m,n}$ as what was called in [JLS2] an ℓ -sharp knot.

Definition 3.15 ([JLS2]). A knot K is ℓ -sharp if $\ell(K) = a(K)$.

There, and later in [St1], various applications of ℓ -sharpness are studied. For example, we also know that alternating knots are ℓ -sharp. (Of course, there are more: all prime knots up to 10 crossings except 10_{132} are ℓ -sharp.)

Here we introduce applications for torus knots, without detailed proofs; for those, we refer to [St1]. However, we emphasize that these proofs sometimes directly follow from ℓ -sharpness, or minor additional conditions, that are ensured from Theorem 1.1.

The first result establishes the equivalence between quasipositivity and strong quasipositivity.

Corollary 3.16. *Assume $K = T_{m,n}$ or $!T_{m,n}$. Then*

- (i) each $C_2(K, t)$ is quasipositive if and only if it is strongly quasipositive,
- (ii) each $W_+(K, t)$ is quasipositive if and only if it is strongly quasipositive, and
- (iii) no $W_-(K, t)$ is quasipositive.

We can also resolve Problem 3.8 for these links.

Corollary 3.17. *Assume $K = T_{m,n}$ or $!T_{m,n}$. Then each $C_2(K, t)$ and $W_{\pm}(K, t)$ is strongly quasipositive if and only if it is Bennequin-sharp.*

Note that for $W_-(K, t)$ this effectively, again, says that it is not Bennequin-sharp for any t . The next consequence addresses Question 3.3 and the existence of a minimal string Bennequin surface.

Corollary 3.18. *Assume $K = T_{m,n}$ or $!T_{m,n}$. Then each $C_2(K, t)$ and $W_{\pm}(K, t)$ has a minimal string Bennequin surface, and if strongly quasipositive, a minimal string strongly quasipositive surface.*

The proof of this property of course relies on determining the braid index.

Corollary 3.19. *Assume $K = T_{m,n}$ or $!T_{m,n}$. Then each $C_2(K, t)$ and $W_{\pm}(K, t)$ is MFW-sharp.*

One can write down explicit formulas. The one for $b(C_2(K, t))$ is simplest, and is an analogue of what Diao and Morton [DM] proved for the alternating knots. This can be obtained by applying (and substituting (49) and (50) into) the below more general result.

Proposition 3.20 ([JLS2]). *Assume K is a non-trivial ℓ -sharp knot. Then*

$$b(C_2(K, t)) = \begin{cases} \lambda(K) - t & \text{if } t \leq \lambda(K) - a(K), \\ a(K) & \text{if } \lambda(K) - a(K) \leq t \leq \lambda(K), \\ t - \lambda(K) + a(K) & \text{if } t \geq \lambda(K). \end{cases} \quad (52)$$

4 Applications to torus links

4.1 Invariants

4.1.1 Arc index

Assume

$$l = (m, n) > 1.$$

The torus link $T_{m,n}$ has l components

of the knot type $T_{m/l, n/l}$. We also maintain throughout the basic assumption

$$n \geq m.$$

Now consider again the braid representation of $T_{m,n}$ as an m -braid of $(m-1)n$ crossings. Its reverse parallel with blackboard framing of each component has l components, each one of framing

$$\left(1 - \frac{m}{l}\right) \frac{n}{l}. \quad (53)$$

Each component K_i of $T_{m,n}$ has linking number

$$lk(K_i, K_j) = \frac{m}{l} \cdot \frac{n}{l} \quad (54)$$

with each other component.

Theorem 4.1. *The arc index for a torus link is $a(T_{m,n}) = m + n$.*

Proof. First notice that the standard grid diagram (51) has its obvious generalization to torus links. We will still refer to this diagram and its planar mirror image as the *standard grid diagram* of a torus link.

Case 1. $l < m$. Then each component $T_{m/l, n/l}$ of $T_{m, n}$ is knotted. So

$$a(T_{m, n}) \geq l \cdot \left(\frac{m}{l} + \frac{n}{l} \right) = m + n.$$

Case 2. $l = m$, so $m \mid n$. All p components of $T_{m, n}$ are unknotted.

Let $k = \frac{n}{m} = \frac{n}{l}$. Each two components of $T_{m, n}$ form a $T_{2, 2k}$, and have a $\geq 2k + 2$ size in a grid diagram of $T_{m, n}$.

Take all 2-component sublinks of $T_{m, n}$, so that each component counts $(m - 1)$ -times. Then

$$\begin{aligned} \text{grid size} &\geq \# \text{ pairs} \cdot \frac{1}{\text{number of times a component counts}} \cdot 2(k + 1) \\ &= \frac{m(m - 1)}{2} \cdot \frac{1}{m - 1} \cdot 2(k + 1) \\ &= m(k + 1) = n + m. \end{aligned}$$

□

4.1.2 Thurston-Bennequin invariants

For a link L of *numbered* components $K_i, i = 1, \dots, l$, let

$$M = L(t_1, \dots, t_l) \tag{55}$$

be the *banded link* of L with framing t_i of the annulus around component K_i . This is the obvious generalization of $C_2(K, t) = K(t)$ for a knot K (and $l = 1$). This construction naturally comes with a particular pairing up of the components of M (with both components in each pair having the same knot type), which we refer to as a *banding structure*. (There is also the suggestive generalization of Whitehead doubles, but for them considerable further complications occur; see §4.3.)

There are a few caveats regarding the links (55) to put up in advance. At least for torus links L , the notation is more or less unambiguous in the following sense.

Lemma 4.2. *The link $T_{m, n}(t_1, \dots, t_l)$, regarded up to isotopy permuting components, determines (t_1, \dots, t_l) up to permutation.*

Proof. Let K_1, \dots, K_{2l} be the $2l$ torus knots of type $T_{m/l, n/l}$ components of

$$M = T_{m, n}(t_1, \dots, t_l).$$

Then when for each fixed K_i , the numbers

$$\{lk(K_i, K_j) : j \neq i\}$$

cancel in pairs (like $\{1, 2, 3, 3, 2\} \mapsto \{1, 3, 3\} \mapsto \{1\}$), and one single number k_i (in the parenthetic example $k_i = 1$) remains. Then (k_1, \dots, k_{2l}) will give each value an even number of times, and by replacing $(k, k) \mapsto k$ (as in $(1, 2, 2, 1) \mapsto (1, 2)$) will give (t_1, \dots, t_l) up to permutations. □

Note, though, that the banding structure of M is not determined uniquely up to isotopy of the collection of bands. This is a point to keep in mind when working with these links.

Example 4.3. Take $M = T_{m, n}(-\frac{n}{l}, \dots, -\frac{n}{l})$ for $l = m$. Then M is the closure of the $2l$ -string braid of n/l full twists, with half of its strands oriented downward. These components are exchangeable, and thus a fixed upward-oriented braid strand bounds a $-\frac{n}{l}$ -framed annulus with every downward-oriented strand. This means that when the $2l$ components of M are numbered, there are at least $l!$ different banding structures on M .

The *component-wise Thurston-Bennequin invariant* of a Legendrian link \mathcal{L} of components \mathcal{K}_i is

$$(TB(\mathcal{K}_1), \dots, TB(\mathcal{K}_l)). \tag{56}$$

Obviously, this is the natural equivalent of the Thurston-Bennequin invariant to study when Legendrian isotopy of Legendrian links is considered. However, almost everywhere simply the extension of (38) seems treated. For links, it yields the much coarser invariant

$$TB(\mathcal{L}) = 2lk(L) + \sum_{i=1}^l TB(\mathcal{K}_i), \quad (57)$$

where $lk(L)$ is the total linking number of L . It is this simplification that occurs in [DP, Ta1, Ta2] for the link case. It allows again for maximizing by setting

$$TB(L) = \max \{ TB(\mathcal{L}) : [\mathcal{L}] = L \}, \quad (58)$$

where brackets denote the underlying topological link type.

Since we like (and often have) to pay attention to component-wise Thurston-Bennequin invariants, we will seek to avoid working in the framework of the above references. In particular, our treatise below seems the first account of extracting information from link polynomials regarding (56) (Theorems 4.5 and 4.9), rather than merely (57). Still, we will treat the latter as well, and for obvious reasons, generalize the notation

$$\lambda(L) = -TB(L). \quad (59)$$

Remark 4.4. We caution that the vector (56) is far more complex to understand than just its short-cut (57). For example, one may be able to reduce

$$\lambda(\mathcal{K}_i) = -TB(\mathcal{K}_i)$$

only at the cost of augmenting some other $\lambda(\mathcal{K}_j)$. The first example we inferred about, using Dynnikov-Prasolov (Theorem 3.12), is the (properly mirrored) Whitehead link: it is exchangeable and has odd arc index. However, we will soon see this problem transpiring even more emphatically for (some) torus links. In particular, maximizing (56) does not seem to make much sense *a priori*. We will return to this issue when we discuss corner framings in §4.4.

Theorem 4.5. *The tuple $(\lambda(\mathcal{K}_1), \dots, \lambda(\mathcal{K}_l))$ realizes the (negated) component-wise Thurston-Bennequin invariants a Legendrian embedding of $T_{m,n}$*

$$\iff \lambda(\mathcal{K}_i) \geq \left(1 - \frac{m}{l}\right) \frac{n}{l} + \frac{m}{l}$$

for all $i = 1, \dots, l$.

We point out, that we do not know (similarly for Theorem 4.9 below) about the strength of (56) for Legendrian torus links. The peculiarities we discover with some negative torus links, though, should serve as serious caveats to extensions of the completeness results for knots [EH]. Of course, this study (including Maslov numbers, etc.) goes beyond our scope and our methods here. However, we at least compensate for the (considerable) loss of information that occurs when replacing (56) by (57).

Proof. \Leftarrow . This can be seen by realizing such an embedding from taking the grid diagram (51) and applying component-wise positive stabilizations. (A *positive stabilization* is the addition of a short horizontal edge at a vertical one creating a pair of NE and SW corners; see (83) and [JLS2, (3.9)].)

\Rightarrow . Every Legendrian embedding gives a Legendrian embedding of the component K_i , which is a $T_{m/l, n/l}$. This Legendrian embedding \mathcal{L} of L gives rise to a grid diagram of L , and thus to a strongly quasipositive band representation of $L(t_1, \dots, t_l)$ where

$$t_i = \lambda(\mathcal{K}_i)$$

with (59).

Each K_i appears in a sub-grid diagram, and thus each $C_2(K_i, t_i)$ has a strongly quasipositive band representation with bands for $K_i = U$. (Here we write the components K_i of L non- calligraphic.) Thus, with (59), we have

$$t_i \geq \lambda(T_{m/l, n/l}) = \left(1 - \frac{m}{l}\right) \frac{n}{l} + \frac{m}{l}.$$

Note that the unknots $K_i = U$ (where $l = m$) are no exception: the right-hand side gives 1. Note that $\lambda(U) = 0$ only due to the existence of the empty band representation of $C_2(U, 0)$, which does not come from a grid diagram of U . \square

Remark 4.6. The existence of the grid diagram is essential in going over to sublinks of L . Obviously every grid diagram of L yields a grid diagram of a sublink of L . But the claim that if a link M is strongly quasipositive then so is a sublink thereof cannot be further from the truth in general; see [St4]. It is only through the grid diagram that we see this property for (the considered sublinks of) $M = L(t_1, \dots, t_l)$.

The consequence below is well known (also more generally, see [Ta2]), but (as indicated above) it is explained here from our setting.

Corollary 4.7. *The Thurston-Bennequin invariant of a torus link is $\lambda(T_{m,n}) = -mn + n + m$.*

Proof. When $\mathcal{T}_{m,n}$ is a Legendrian embedding of $T_{m,n}$, then

$$\begin{aligned}\lambda(\mathcal{T}_{m,n}) &= -2\text{lk}(T_{m,n}) + \sum \lambda(\mathcal{K}_i) \\ &\geq -2 \cdot \left(\frac{l(l-1)}{2} \cdot \frac{m}{l} \cdot \frac{n}{l} \right) + \left(l \cdot \left(1 - \frac{m}{l} \right) \cdot \frac{n}{l} + m \right) \\ &= -\frac{mn(l-1)}{l} + n - \frac{mn}{l} + m \\ &= -mn + n + m,\end{aligned}$$

and equality is realizable because for the minimal $\lambda(\mathcal{K}_i)$ we can have equality in the second row. \square

Now let us move to $!T_{m,n}$, the far more interesting case. First, we make a few remarks on $l = (m,n) = 1$, the torus knots. They have the negative braid representation of $(m-1)n$ crossings. We have

$$\lambda(!T_{m,n}) = mn.$$

Since

$$\lambda(!\mathcal{T}_{m,n}) \geq mn = n + (m-1)n,$$

we need in the blackboard framed $\uparrow\downarrow$ parallel (with framing $(m-1)n$) at least n extra positive full twists of each band for a strongly quasipositive band representation.

When we go over to links $T_{m,n}$, one can still apply the reasoning on the components $T_{m/l,n/l}$, *unless* they are unknotted, i.e., $m = l$. This case (as already apparent from the proof of Theorem 4.1) will continuously require extra considerations below, thus let us set up the following terminology.

Definition 4.8. We call a (m,n) -torus link *pure* if $m \mid n$ (i.e., $l = m$), and *non-pure* otherwise.

Keeping this in mind, for $l = (m,n) > 1$, we formulate the complete description of component-wise Thurston-Bennequin invariants of negative torus links.

Theorem 4.9. *Assume*

$$(t_1, \dots, t_l) = (\lambda(\mathcal{K}_1), \dots, \lambda(\mathcal{K}_l)) \tag{60}$$

are the (negated) component-wise Thurston-Bennequin invariants a Legendrian embedding $!\mathcal{T}_{m,n}$ of $!T_{m,n}$.

(i) *If $T_{m,n}$ is non-pure, then the occurring tuples (60) are exactly described, for all $i = 1, \dots, l$, by the condition*

$$t_i \geq \frac{m}{l} \cdot \frac{n}{l}. \tag{61}$$

(ii) *If $T_{m,n}$ is pure, then for $k = n/m$, the occurring tuples (60) are exactly described by one of the two following conditions:*

(a) *Either*

$$t_i \geq k \tag{62}$$

for $i = 1, \dots, l$.

(b) *Or $k > 1$, and there is a number $1 \leq u < k$ and a component K_{i_0} so that*

$$t_{i_0} = u \quad \text{and} \quad t_i \geq 2k - u \tag{63}$$

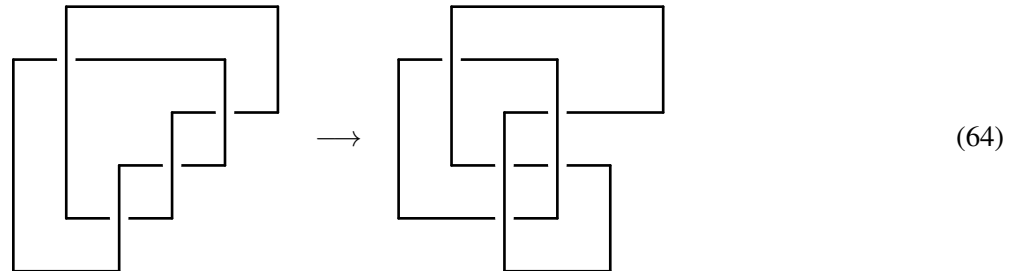
for all $i = 1, \dots, l$ with $i \neq i_0$.

Obviously, inequality (62) is the special case of (61) when $l = m$. The tuples (63) will be called below *auxiliary framings*. (The term ‘framings’ refers to t_i manifesting themselves as the framings of the annulus link obtained from the grid diagram of the Legendrian embedding using the grid-band construction of §3.3 – where of course only positive bands are used.)

We also add the following technical remarks. Be aware that $!\mathcal{T}_{m,n}$ is a notation. A Legendrian embedding of $!T_{m,n}$ is not simply the mirror image of a Legendrian embedding of $T_{m,n}$. Furthermore, we assume the mirror image operator $!$ to bind stronger than the banding operation $L \mapsto L(\dots)$. That is, $!L(t_1, \dots, t_l)$ is understood as parenthesized like $(!L)(t_1, \dots, t_l)$, and not as $!(L(t_1, \dots, t_l)) = (!L)(-t_1, \dots, -t_l)$.

Proof. \Leftarrow Take the planar mirror image of (51) for a minimal grid diagram of $!T_{m,n}$, and apply component-wise positive stabilizations (see the proof of Theorem 4.5). This deals with realizing (61) and (62).

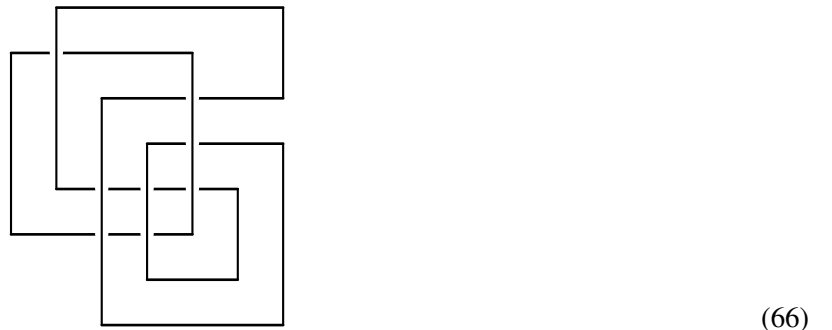
To handle (63), first let $m = 2$. Consider the following example of 6-grid diagram of the negative $(2,4)$ -torus link, which is shown on the right of (64).



The link, $!T_{2,2}(1,3)$, obtained from the grid-band construction with positive bands, is shown below.



One can understand the grid diagram yielding (65) as the result of application of a move (64) on the standard diagram, which can be iteratively generalized. The example for $(2,6)$ -torus link explains how to proceed for a general $(2,2k)$ -torus link.



To move from this to a $(m,mk) = (m,n)$ -torus link, notice that it is obtained from the $(2,2k)$ -torus link by $m-1$ -cabling (any) one of the components with k negative full twists. And we leave it to the reader to convince

themselves that this cabling operation can be applied (with this appropriate number of full twists) to the component in (66) with self-crossings, so that each segment of its grid is replaced by $m - 1$ segments.

⇒ Each Legendrian embedding $!T_{m,n}$ with Thurston-Bennequin invariant $(TB(\mathcal{K}_1), \dots, TB(\mathcal{K}_l))$ gives rise to a grid diagram of $!T_{m,n}$ and a strongly quasipositive band representation of $!T_{m,n}(t_1, \dots, t_l)$, with

$$t_i = \lambda(\mathcal{K}_i).$$

In particular, this gives a strongly quasipositive band representation of each component $K_i(t_i) = C_2(K_i, t_i)$.

If $K_i \neq U$, which is when $l < m$, then

$$t_i \geq \lambda(T_{m/l, n/l}) = \frac{m}{l} \cdot \frac{n}{l},$$

and we are done. Thus we deal henceforth only with the (far more involved) pure link case that

$$l = m \text{ and } K_i = U.$$

To proceed, consider the 2-component sublink of $!T_{m,n}$, which is of type $M := !T_{2,2k}$, for $k = n/m$. The link $!T_{m,n}(t_1, \dots, t_l)$ must be strongly quasipositive, and yields a strongly quasipositive sublink $M(t_1, t_2)$ (with the caveat of Remark 4.6), for any choice of a two-component sublink $!T_{2,2k}$ of $!T_{m,n}$. (Compare with the link in (65), which occurs for $t_1 = 1, t_2 = 3$ and $k = 2$.)

Note that making annuli from the blackboard framing of the closed negative braid $\sigma_1^{-2k} \in B_2$ yields $M(0,0)$.

Let $n' = 2k$. Then Theorem 2.34 shows that

$$\min \deg_v P(M(0,0)) = 1 - 2n' = 1 - 4k.$$

(This special case, for $m = 2$, can be also proved with a similar skein-algebra tour-de-force as for odd n' in [JLS2].)

By a sublink argument, using the grid diagram (and again being aware of the Remark 4.6), we need that

$$\text{when } M(t_1, t_2) \text{ is strongly quasipositive, then } t_i > 0. \quad (67)$$

Thus we can assume that only positive twists are added in the bands of $M(0,0)$ (like at the bottom of the previously recalled example in (65)).

Now, when a crossing is smoothed out in $U(t_1)$, we get the split union of U and $U(t_2)$ for $t_2 > 0$. This does not affect P -terms of negative v -degree. Therefore,

$$\min \deg_v P(M(t_1, t_2)) = 1 - 4k + 2(t_1 + t_2)$$

for $t_1 + t_2 < 2k$. This means that

$$\min \deg_v P(M(t_1, t_2)) < 0. \quad (68)$$

Now

$$\chi(M(t_1, t_2)) = 0, \quad (69)$$

since $M(t_1, t_2)$ bounds two annuli, but not a Seifert surface with a disk component ($M(t_1, t_2)$ has no split unknotted component).

Thus if $M(t_1, t_2)$ is strongly quasipositive, then $\min \deg_v P(M(t_1, t_2)) > 0$. Hence, from (68),

$$t_1 + t_2 \geq 2k = n'. \quad (70)$$

This gives then the claim: if all $t_i \geq k$, then for each 2-component sublink of $!T_{m,n}$, the condition (70) holds, and we have (61). Otherwise, let $0 < t_1 =: u < k$. We have then that $t_2 \geq 2k - u$ for any choice of component K_2 different from K_1 . Thus we have (62). □

Corollary 4.10. *The Thurston-Bennequin invariant of the mirror image is $\lambda(!T_{m,n}) = mn$.*

For this consequence of Theorem 4.9 we can resort to (70).

Proof. For non-pure $!T_{m,n}$,

$$\begin{aligned}\lambda(!T_{m,n}) &\geq \sum_i \lambda(K_i) - 2 \sum_{i < j} lk(K_i, K_j) \\ &= \left(l \cdot \frac{m}{l} \cdot \frac{n}{l} \right) + 2 \cdot \frac{m}{l} \cdot \frac{n}{l} \cdot \frac{l(l-1)}{2} \\ &= \frac{mn}{l} + mn - \frac{mn}{l} = mn.\end{aligned}$$

Here, in the first row now $lk(K_i, K_j)$ changes sign from (54) due to the mirroring.

For pure $!T_{m,n}$, one can still justify the first pair of parentheses in the second row by averaging out over all pairs of components K_i, K_j of $!T_{m,n}$, using (70). \square

Note that this corollary can be obtained also from Dynnikov-Prasolov and Theorem 4.1 and Corollary 4.7. But, again, we only allude to, and do not invoke their framework here.

4.2 Geometric properties

4.2.1 Arc index revisited

With Theorem 4.1 and Theorem 2.34, we see that the ℓ -invariant (47) does yield the correct value for the arc index. However, this invariant cannot be applied straightforwardly to links. The aim of the exposition here is to use torus links as a starting example for generalizing the techniques underlying the ℓ -invariant to links. This will also suggest ways how to extend the ℓ -invariant itself (§4.4).

We continue using the banding of the blackboard framing of $T_{m,n}$ as a positive m -braid of $(m-1)n$ crossings. One has l components, each with framing

$$\delta := \left(1 - \frac{m}{l} \right) \frac{n}{l}. \quad (71)$$

Since the shift of framing by δ will be so common below, we introduce the following extra notation to save writing.

Definition 4.11. Let us say (e_1, \dots, e_l) is the *corrected framing* if $(\delta + e_1, \dots, \delta + e_l)$ is the real framing. Write

$$\tilde{T}_{m,n}(e_i)_i = T_{m,n}(\delta + e_i)_i$$

for the banding link of $T_{m,n}$ with corrected framing $(e_i)_i$.

Then Theorem 2.34 implies that

$$\max \deg_v P(\tilde{T}_{m,n}(0, \dots, 0)) = 2n - 1.$$

Corollary 4.12. The maximum degree of the torus link with corrected framing is given by

$$\max \deg_v P(\tilde{T}_{m,n}(e_1, \dots, e_l)) = 2n - 1 + 2 \sum_{i=1}^l e_i$$

when all $e_i \geq 0$.

Proof. We perform induction over

$$\left(l, \sum_{i=1}^l e_i \right),$$

using the skein relation (5) applied at a positive crossing of $\tilde{K}_i(e_i)$,

$$P(\tilde{T}_{m,n}(e_1, \dots, e_l)) = vzP_0 + v^2P_- . \quad (72)$$

Note that when deleting a component $\tilde{K}_i(e_i)$ of $\tilde{T}_{m,n}(e_1, \dots, e_l)$, one obtains

$$\tilde{T}_{m(l-1)/l, n(l-1)/l}(e_1, \dots, e_{i-1}, e_{i+1}, \dots, e_l). \quad (73)$$

Thus P_0 in (72) is the polynomial of the split union of (73) and an unknot U , and P_- is the polynomial of

$$\tilde{T}_{m,n}(e_1, \dots, e_{i-1}, e_i - 1, e_{i+1}, \dots, e_l).$$

Using that

$$n(l-1)/l < n \quad (74)$$

and induction on the number of components l for the P_0 term, and induction over $\sum_{i=1}^l e_i$ for the P_- term, we see that the leading v -degree term of $v^2 P_-$ in (72) is always of higher v -degree than the leading v -degree term of vzP_0 . \square

Corollary 4.13. *The arc index is given by $a(T_{m,n}) = m + n$.*

The point of repeating this result is that now we emphasize a technique that leads later to extending the ℓ -invariant (§4.4), and builds more on the HOMFLY-PT polynomial's own capacity, than on sublink arguments.

Proof. Assume there is a grid diagram of $T_{m,n}$. This gives, via the grid-band construction, a strongly quasipositive banding link $M = \tilde{T}_{m,n}(e_i)_i$, where we need

$$e_i \geq \frac{m}{l} \quad (75)$$

because of strong quasipositivity of components. (We will deal with the auxiliary framings extra below.) We have, by applying (18) as in the proof of Theorem 2.34, and degree shift from linking numbers,

$$\min \deg_v [P(M)]_{z^{1-2l}} = 1,$$

when all $e_i = \frac{m}{l}$. Thus, by (further) switch of linking numbers

$$\min \deg_v [P(M)]_{z^{1-2l}} = 1 + 2 \sum_{i=1}^l \left(e_i - \frac{m}{l} \right)$$

for e_i in (75). By Corollary 4.12,

$$\max \deg_v P(M) = 2n - 1 + 2 \sum_{i=1}^l e_i. \quad (76)$$

Then

$$\begin{aligned} 2\text{MFW}(M) - 2 &\geq \max \deg_v P(M) - \min \deg_v [P(M)]_{z^{1-2l}} \\ &= 2n - 1 + 2m - 1 = 2m + 2n - 2. \end{aligned}$$

Now note that for the auxiliary framings (of pure links) the argument applies as well. Thus

$$\text{MFW}(M) \geq m + n.$$

Hence, every strongly quasipositive banding link of $T_{m,n}$ has braid index at least $m + n$. This gives $a(T_{m,n}) \geq m + n$, with the reverse inequality being obvious from (51). \square

4.2.2 Minimal string strongly quasipositive surfaces

Corollary 4.14. *Let M be a strongly quasipositive banding of $T_{m,n}$ with corrected framing (e_1, \dots, e_l) for (75). Then the braid index is*

$$b(M) = n + \sum_{i=1}^l e_i.$$

Proof. We use (76) and

$$\text{“} \min \deg_v P(M) = 1 \text{”}. \quad (77)$$

We do not know whether this is always true, but it can be assumed true for braid index purposes, because of Bennequin's inequality and

$$\chi(M) = 0$$

(with the same argument as for (69)). Thus, even if (77) is not true, we can always assume it true for estimating $b(M)$ using $\text{MFW}(M)$ from (40). With this justification, (76) and (77) gives

$$b(M) \geq \text{“MFW}(M)\text{”} = \frac{1}{2}(\max \deg_v P(M) - \text{“mindeg}_v P(M)\text{”}) + 1 = n + \sum_{i=1}^l e_i. \quad (78)$$

The reverse inequality holds, because one can find a grid diagram of $T_{m,n}$ with $\lambda(K_i) = \delta + e_i$ (see (71)) by using component-wise positive stabilization of the standard grid diagram (51). This process yields a grid diagram of the size being the right-hand side of (78). \square

Corollary 4.15. *If M is a strongly quasipositive banding link of $T_{m,n}$, then M has a minimal string strongly quasipositive surface.*

The problem to determine the braid index (and minimal string Bennequin surface) of an arbitrary banded link of $T_{m,n}$ remains more complex. We suspect that, if Diao-Morton type of formulas (52) hold for braid indices of bandings of (even only torus) links, they will be very involved, and it is extremely difficult to control degeneracies (even in our special cases).

Now consider the mirror $!T_{m,n}$. Every component is $!T_{m/l,n/l}$, and the minimal strongly quasipositive annulus framing is $\frac{mn}{l^2}$ unless $m = l$ (where we have the constructions (64),(66) of auxiliary framings). Recall Theorem 4.9.

Theorem 4.16. *Assume $M = !T_{m,n}(t_1, \dots, t_l)$ is a strongly quasipositive banding of $!T_{m,n}$. Then M has a minimal string strongly quasipositive surface.*

While again one can use sublinks, the argument here relies more on the capacity of P itself, assisted by Bennequin's inequality through (77). We see again that they are sufficient to determine the braid index of M .

Proof. We observe again from Theorem 2.34, by taking the mirror image (and, modulo coefficient signs, v to v^{-1}), that

$$!T_{m,n}(\kappa, \dots, \kappa), \quad \kappa = \left(\frac{m}{l} - 1\right) \cdot \frac{n}{l}$$

(note the change of sign in (53)) had

$$\max \deg_v [P]_{z^{1-2l}} = 2m - 1.$$

It follows, by just changing linking numbers, that

$$M_0 = !T_{m,n} \left(\frac{mn}{l^2}, \dots, \frac{mn}{l^2} \right)$$

has

$$\max \deg_v [P(M_0)]_{z^{1-2l}} = 2(m+n) - 1.$$

Then

$$\max \deg_v [P(!T_{m,n}(t_1, \dots, t_l))]_{z^{1-2l}} = 2(m+n) - 1 + 2 \sum_{i=1}^l \left(t_i - \frac{mn}{l^2} \right)$$

for $t_i \geq \frac{mn}{l^2}$, by linking number reasons.

With (77), we have

$$b(M) \geq \text{“MFW}(M)\text{”} = m+n + \sum_{i=1}^l \left(t_i - \frac{mn}{l^2} \right). \quad (79)$$

Conversely, M does have a braid (band) representative on (right-hand side of (79)) strands, by the grid-band construction applied on the appropriate positive stabilization of the mirrored diagram (51).

Thus the braid index of M is given by right-hand side of (79), and M has a strongly quasipositive braid representative on that many strands.

The auxiliary framings (for the pure torus links) can be handled similarly, and we leave them to the reader. \square

The idea in this proof is that one can adapt the definition of ℓ as an arc index bound of a l -component link L , when one replaces $\max \deg_v P$ of strongly quasipositive banded links of L by $\max \deg_v [P]_{z^{1-2l}}$. This is an alternative path to considering (banded links of) sublinks of L . (See further §4.4.)

As for $T_{m,n}$, it is (equally and) too complicated to consider the braid index and Bennequin surface of an arbitrary banded link of $!T_{m,n}$.

4.2.3 Bennequin sharpness

Here we can extend the Bennequin sharpness results and, partially, the equivalence of quasipositivity and strong quasipositivity.

Theorem 4.17. *Let $L = T_{m,n}$ or $!T_{m,n}$. Assume $M = L(t_1, \dots, t_l)$ is Bennequin-sharp. Then it is strongly quasipositive.*

Proof. The idea in both cases is to see that Bennequin sharpness of M restricts t_i to be as in Theorems 4.5 and 4.9. The theorems then say (via the grid-band construction) that M is strongly quasipositive.

Let us write below $w(\beta)$ for the writhe (exponent sum) of a braid $\beta \in B_r$ and $r = r(\beta)$ for its string number.

(i) $L = !T_{m,n}$. If $L = L_1 \cup L_2$, where L_i are l_i -component sublinks of L , then

$$M = M_0 = L(t_1, \dots, t_l) = M_1 \cup M_2$$

with

$$M_1 = L_1(t_1, \dots, t_{l_1}), \quad M_2 = L_2(t_{l_1+1}, \dots, t_l).$$

Again, M_i have no split unknots, so $\chi(M_i) = 0$ (with the same argument as for (69)). Also

$$lk(M_1, M_2) = 0$$

in M . We will argue, in (81), that a braid β with $\hat{\beta} = M$ making M Bennequin sharp, splits into subbraids β_i with $\hat{\beta}_i = M_i$ making M_i Bennequin sharp.

When $l < m$, then argue with 1-component sublinks of M , analogously to the case $l = m$ that just follows.

For the case $l = m$, use 2-component sublinks. As below, we see that a 2-component banded sublink

$$Y = !T_{2,n'}(t_1, t_2)$$

for $(n' = 2n/l)$ is Bennequin sharp implies that

$$t_1 + t_2 \geq n', \quad t_i > 0. \quad (80)$$

Namely, since $\chi(Y) = 0$, assume that

$$Y \text{ has a braid representative } \beta \text{ with } w(\beta) = r(\beta).$$

Thus β has subbraids $\beta_{1,2}$ with $\hat{\beta}_i = C_2(U, t_i) = U(t_i)$.

We claim, for $i = 1, 2$,

$$w(\beta_i) = r(\beta_i). \quad (81)$$

Since $lk(U(t_1), U(t_2)) = 0$, we have

$$w(\beta_1) + w(\beta_2) = w(\beta),$$

and obviously also

$$r(\beta_1) + r(\beta_2) = r(\beta) = w(\beta).$$

If $w(\beta_i) > r(\beta_i)$ for some $i = 1, 2$, then we would have a contradiction to Bennequin's inequality for $U(t_i)$, since $-\chi(U(t_i)) \leq 0$ (even if $t_i = 0$, the argument works). Thus (81) holds.

To obtain (80), we checked in (68) that

$$\min \deg_v P(Y) < 0$$

when $t_1 + t_2 < n'$, and also it is easy to directly verify that

$$\min \deg_v P(U(t_i)) < 0$$

when $t_i \leq 0$. This shows (80) and leads as before to (62) and (63).

(ii) $L = T_{m,n}$. This is easier.

If $l < m$, use the sublink argument to establish that $K_i(t_i)$ must be Bennequin sharp. This yields the restriction in Theorem 4.5,

$$t_i \geq \left(1 - \frac{m}{l}\right) \frac{n}{l} + \frac{m}{l},$$

by using the result for torus knots in Theorem 4.17.

If $l = m$, we still need $t_i \geq 1$ (and not only $t_i \geq 0$), since any sublink $U(t_i)$ of M banding an unknotted component of L cannot yield a split unknot of M . \square

Corollary 4.18. *Assume $l < m$, i.e., $T_{m,n}$ is non-pure. Then $L = T_{m,n}(t_1, \dots, t_l)$ or $!T_{m,n}(t_1, \dots, t_l)$ is strongly quasipositive if and only if it is quasipositive.*

Proof. We have $\chi_4(L) = 0$, since the components of $T_{m,n}$ are knotted (and not slice) and none bounds a disk even in B^4 . Thus

$$\text{quasipositive} \implies \text{Slice-Bennequin-sharp} \implies \text{Bennequin-sharp} \implies \text{strongly quasipositive}.$$

When $L = T_{m,n}$ for $l = m$, and $K_i = U$, then $M = L(t_1, \dots, t_l)$ for $t_i = 0$ has

$$\chi_4(M) = 2.$$

(Even if there are multiple $K_i = U$ with $t_i = 0$, one cannot span more than two slice disks into unknotted components of M due to linking number reasons.) But

$$\chi_4(M) > \chi(M) \tag{82}$$

breaks down the previous proof. This suggests how to find the next example, showing that Corollary 4.18 is indeed false for pure torus links.

Example 4.19. The link $M = T_{2,2}(0, 1)$ has the 4-braid representative

$$[-1 \ -2 \ -3 \ -2 \ 1 \ 3 \ -2 \ \underline{3} \ 2 \ -1 \ 2 \ 1 \ 3 \ 2].$$

It is quasipositive, as can be seen when deleting the underlined letter and showing that the remainder of the word is conjugate to the last letter σ_2 . Thus M is quasipositive, but because of (82), certainly not strongly so.

One can, of course, in many cases still use the HOMFLY-PT polynomial to obstruct to quasipositivity of M through explicit calculations. But this becomes too hard to control in the general form. (When $l = 1$, then of course this troublesome case reduces to the trivial case.) When $t_i \neq 0$ whenever $K_i = U$, then the argument for the corollary can still be used, though.

Similarly to Remark 4.6, looking at sublinks is completely useless in studying quasipositivity (see [BD]).

Even beyond the auxiliary framings, the difficulties with pure torus links here are nothing unexpected. One should by no means assume that the equivalence of quasipositivity and strong quasipositivity is something natural or even common. There are myriads of instances where it fails. We highlight that even for knots K , these properties of $C_2(K, t)$ do not coincide (see [St1]), and thus such pathologies can only worsen with more components. Also here, the question when our links M are quasipositive remains at least partially unresolved.

4.2.4 The Baker-Motegi problem

A related problem on strong quasipositivity, raised by Baker and (independently) Motegi is as follows.

Problem 4.20. (Baker-Motegi) Assume a link M is strongly quasipositive. Is every maximal χ surface of M strongly quasipositive?

For instance, this problem was resolved for canonical surfaces in [St2], but our surfaces here are surely highly non-canonical. The problem was not discussed in [JLS2] since, when L is a knot, the maximal χ surface of M is unique (which makes the problem trivial). However, Example 4.3 shows that links L are far more subtle. We can now state the following.

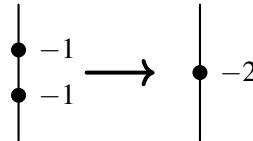
Theorem 4.21. *Assume L is a torus link (positive or negative) and $M = L(t_1, \dots, t_l)$ is strongly quasipositive. Then every maximal χ surface of M is strongly quasipositive.*

Proof. Let S be a maximal χ surface of M . Since M bounds a collection of annuli, but has no split unknotted components, $\chi(M) = 0$, and thus S is a collection of annuli. This means that S determines a banding structure of $M = L(t_1, \dots, t_l)$.

By Rudolph [Ru1], S is a braided surface, and thus arises from the grid-band construction on a grid diagram D' of L , but with possibly negative bands.

Let $t'_i = \lambda(K'_i)$ for the components K'_i of the grid diagram D' . Obviously $t'_i - t_i$ is the number of negative bands of component K'_i , which are smashed into vertical segments by reversing the grid-band construction.

We correct now the negative bands by introducing a *beaded grid diagram* (and extending grid-band construction to this slightly more general case). On each horizontal segment a bead with an integer label ξ is allowed, meaning that at this point the band in the grid-band construction (now mandatorily positive) experiences ξ full twists (positive, or $-\xi$ negative if $\xi < 0$). Obviously a bead with zero label can be deleted (or created), and beads on the same vertical segment can be joined (through an isotopy of the surface S).



For instance, the following modifies the positive stabilization as an isotopy of S .



Note that it is an isotopy of the surface S to move a bead from top to bottom of a vertical segment (a flype at the band crossing), and similarly to move beads across horizontal segments of the same component of L (flypes at the braid string disk).

Now, by Lemma 4.2, the tuple (t_1, \dots, t_l) is unique up to permutations, and thus must satisfy the restrictions of Theorem 4.9.

By the proof of Theorem 4.9, there must exist a sequence of Cromwell moves [AHT] turning our above grid diagram D' into one D whose components K_i have $t_i = \lambda(K_i)$.

But this sequence of Cromwell moves obviously extends to a sequence of Cromwell moves of beaded diagrams: each time a Cromwell move changes the TB invariant of a component C , a bead can be put on some of the vertical segments of C to correct for that change.

These Cromwell moves of beaded diagrams then yield isotopies of the surface S . (The beaded positive stabilization (83) above is an example.) And at the end (the labels of) all beads on every component of D must cancel out. Thus S is isotopic to the (strongly quasipositive) surface that is obtained by the grid-band construction applied on D , now with positive bands only. \square

Remark 4.22. Note that, when combined with §4.2.2, this proof yields the following sharper property than the results there: if $M = T_{m,n}(t_1, \dots, t_l)$ or $M = !T_{m,n}(t_1, \dots, t_l)$ is strongly quasipositive, then *every* strongly quasipositive surface of M is realizable on a minimal string braid of M .

It is tempting to speculate (see [JLS2]) whether this property holds for any strongly quasipositive link M , but it appears unlikely.

4.3 Whitehead doubled links

Another application returns to the Whitehead doubling (see beginning of §4.1.2). Let us write

$$M = L(t_1^\pm, \dots, t_l^\pm) \tag{84}$$

by indicating both framing and clasp for each component of L . Thus $L(t_1^+) = W_+(L, t_1)$ and $L(t_1^-) = W_-(L, t_1)$ in the previous notation.

We only state the following theorem. Its proof is a longer (and tricky) amalgamation of further tools (including cut-and-paste arguments and concordance invariants), and goes slightly beyond the style (and volume) of this paper. (It is available upon request).

Theorem 4.23. *The link $M = L(t_1^\pm, \dots, t_l^\pm)$ is strongly quasipositive if and only if all clasps are positive, and (t_1, \dots, t_l) satisfy the restrictions of Theorem 4.5 for $L = T_{m,n}$ resp. Theorem 4.9 for $L = !T_{m,n}$.*

The following, now less startling, example warns again that understanding the quasipositivity of the links M is likely very difficult, even when L is a torus link.

Example 4.24. Example 4.19 can be modified with some care to yield a 4-braid representative of $M = T_{2,2}(0^+, 1^+)$,

$$[-1 \ -2 \ -3 \ -2 \ 1 \ 3 \ -2 \ 3 \ 3 \ 2 \ -1 \ 2 \ 2 \ 1 \ 3 \ 2].$$

This link (which consists of an unknot and a right-hand trefoil component) is thus quasipositive and $\chi_4(M) = 0$. But the proof of Theorem 4.23 does yield that for strongly quasipositive M ,

$$\chi(M) = -l. \tag{85}$$

With $l = 2$, this would again give (82). Therefore (even without invoking Theorem 4.23 directly), we see that M cannot be strongly quasipositive.

Remark 4.25. With a similar combination of a variant of Corollary 4.12 and the Bennequin bound (77), it is not too difficult to argue that the links M of Theorem 4.23 have a minimal string strongly quasipositive surface. (Use (85) as in (77).) However, the resolution of Problem 4.20 (i.e., an analogue of Theorem 4.21) remains beyond reach.

4.4 Generalizing the ℓ -invariant for arbitrary links

Here we extend some of the previous ideas mostly used for torus links to general links L . For links, far more technical considerations need to be made than for knots.

Fundamental assumption: L has no trivial split components.

Definition 4.26. Assume L has numbered components K_i for $i = 1, \dots, l$. The *framing cone* of L is

$$\Omega(L) := \{(t_1, \dots, t_l) : L(t_1, \dots, t_l) \text{ is strongly quasipositive}\}.$$

For reasons already explained (and with the above fundamental assumption),

$$\Omega(L) = \left\{ (t_1, \dots, t_l) : \begin{array}{l} \text{There is a Legendrian embedding} \\ \mathcal{L} \text{ of } L \text{ with } (\lambda(\mathcal{K}_i))_{i=1}^l = (t_i)_{i=1}^l \end{array} \right\}.$$

Because of positive stabilization, if $(t_1, \dots, t_l) \in \Omega(L)$, then

$$\left(\prod_{i=1}^l [t_i, \infty) \right) \cap \mathbb{Z}^l \subset \Omega(L).$$

Let

$$C(t_1, \dots, t_l) := \left(\prod_{i=1}^l [t_i, \infty) \right) \cap \mathbb{Z}^l.$$

Definition 4.27. When

$$\Omega(L) = \bigcup_j C(t_{1,j}, \dots, t_{l,j}),$$

so that the union of no proper subfamily of $\{C(t_{1,j}, \dots, t_{l,j})\}_j$ covers $\Omega(L)$, we say that $(t_{1,j}, \dots, t_{l,j})$ are *corner framings* of L .

The set of corner framings of L is uniquely determined up to permutation (as easy but slightly tedious exercise).

Example 4.28. Theorems 4.5 and 4.9 say that $T_{m,n}$ has the single corner framing (α, \dots, α) for

$$\alpha = \left(1 - \frac{m}{l}\right) \frac{n}{l} + \frac{m}{l}. \quad (86)$$

When $m \nmid n$, then $!T_{m,n}$ has the single corner framing (γ, \dots, γ) for

$$\gamma = \frac{mn}{l^2}.$$

Otherwise, for $k = n/m$, it has a set of corner framings

$$(u, 2k-u, \dots, 2k-u), \quad (87)$$

for any $1 \leq u \leq k$, plus (if $u < k$, cyclic) permutations thereof.

One can easily argue (using the existence of an admissible framing; see Definition 4.29 and Example 4.31) that corner framings for every fixed link L are finitely many. But even a (pure) torus link can thus have an arbitrarily large number of them. Another series of examples are connected sums of Whitehead links. (We were aware of them based on Remark 4.4, before identifying the pure torus links.)

A further consequence of the auxiliary framings (87) (for $u < k$) is that corner framings need not realize the minimal total invariant $\lambda(L)$ from (59).

We do not know whether under some extra assumptions (like L being alternating³), such peculiarity can be avoided. However, there is enough evidence that no simple description of corner framings will be available for most links L .

Definition 4.29. Let us say that

$$\phi = (t_1, \dots, t_l) \succeq \phi' = (t'_1, \dots, t'_l)$$

if $t_i \geq t'_i$ for all $i = 1, \dots, l$, and we call ϕ a *stabilization* of ϕ' . We say that a framing (c'_1, \dots, c'_l) of L is *admissible* if $(c'_1, \dots, c'_l) \preceq (e_1, \dots, e_l)$ for every corner framing (e_1, \dots, e_l) of L or, in other words, if

$$\Omega(L) \subset C(c'_1, \dots, c'_l).$$

Example 4.30. If $l = 1$ (so L is a knot) and assuming

$$\lambda(U) = 1, \quad (88)$$

then $\phi = (t)$ is admissible if and only if $t \leq \lambda(L)$.

Example 4.31. Note in particular that $\lambda(L) := (\lambda(K_1), \dots, \lambda(K_l))$ is always admissible, where we are also allowed to set (88) due to the fact we always consider strongly quasipositive band representations of $U(t_i)$ with bands. (Here the assumption also enters that L has no trivial split components.) Consequently also all $\phi \preceq \lambda(L)$ are admissible.

³Note that we do need $m > 2$ for a torus link in order this scenario to occur.

In some attempt to generalize the reasoning for $L = T_{m,n}$, we formulate some ideas that lead to a different version of the ℓ -invariant for links.

Definition 4.32. (i) We say that $(\emptyset = L_0, L_1, \dots, L_l)$ is a *flag of sublinks* of L , if $L_l = L$ and each L_{i-1} is obtained from L_i by deleting exactly one component of L_i .

(ii) We adapt this notion to bandings of L , by saying $M_{i-1} = L_{i-1}(c_{i-1,1}, \dots, c_{i-1,i-1})$ is obtained from $M_i = L_i(c_{i,1}, \dots, c_{i,i})$ by deleting the 2 components of $K_{i,j_i}(t_{i,j_i})$, for some $1 \leq j_i \leq i$, so that

$$(c_{i-1,1}, \dots, c_{i-1,i-1}) = (c_{i,1}, \dots, c_{i,j_i-1}, c_{i,j_i+1}, \dots, c_{i,i}).$$

(iii) We say that a flag $(\emptyset = M_0, \dots, M_l = M)$ of banded sublinks is *P-increasing* if

$$\max \deg_v P(M_i) > \max \deg_v P(M_{i-1}), \quad (89)$$

for each i , with the stipulation $\max \deg_v P(\emptyset) := 0$.

While the condition looks technical, keep in mind that it is a finite number of inequalities (89). It can be easily seen that their number is the same as the number of edges in the 1-skeleton of the l -dimensional cube, which is $l2^{l-1}$.

Theorem 4.33. Let L have an admissible framing ϕ , so that each flag of banded links of $M = L(\phi)$ is *P-increasing*. Then

$$\ell_0(L) := \min_{\kappa \text{ corner framing}} \frac{1 + \max \deg_v P(L(\kappa))}{2}$$

satisfies

$$a(L) \geq \ell_0(L).$$

Proof sketch. We only outline the argument, as it mostly repeats reasoning rolled out for the torus links.

The idea is to use sublinks as in the proof of Corollary 4.12, and the Bennequin inequality constraint (77). The preceding remark also clarifies that κ are finitely many, thus no problem occurs building the minimum.

(The condition of M being *P-increasing* implies that the expressions minimized over are positive.) \square

Example 4.34. We write ℓ_0 to emphasize that for knots K , not always $\ell_0 = \ell$. For example $\ell(10_{132}) = 8$, but with $\lambda(10_{132}) = 1$ (which, in passing by, also fixes our mirroring for the knot), we have $\max \deg_v P(C_2(10_{132}, 1)) = 17$, thus $\ell_0(10_{132}) = 9$.

However, it is true that

$$\ell_0(K) \geq \ell(K), \quad (90)$$

and we invite the reader to think about it (see below Example 4.36).

A more practical modification, which does not require one to know the corner framings, is the following.

Theorem 4.35. Let L have an admissible framing ϕ , so that each flag of banded links of $M = L(\phi)$ is *P-increasing*. Then

$$\ell_\phi(L) := 1 + \frac{\max \deg_v P(L(\phi)) - \min(1, \min \deg_v [P(L(\phi))]_{z^{1-2l}})}{2}$$

satisfies

$$a(L) \geq \ell_\phi(L).$$

Proof sketch. This uses that $[P(M)]_{z^{1-2l}}$ just shifts with change of linking numbers (see the proof of Theorem 4.16). \square

Example 4.36. This bound clearly depends on ϕ . For example, if $L = 10_{132}$ and $\phi = (0)$, then $\ell_\phi(L) = \ell(L) = 8$, but as we saw, if $\phi = (1)$, then $\ell_\phi(L) = 9$.

We leave it as an exercise to the reader to see that when $L = K$ is a knot, and

$$\phi = (\theta(K)),$$

with (48), which can be rephrased as

$$\theta(K) = \min\{t \in \mathbb{Z} : \min \deg_v P(C_2(K, t)) > 0\},$$

then $\ell_\phi(K) = \ell(K)$ recovers the ℓ -invariant (47) of knots. (In the above example $\theta(10_{132}) = 0$.) This argument also easily shows that

$$\ell(L) \leq \ell_\phi(L), \tag{91}$$

for a knot K , whatever admissible framing ϕ is chosen. This relates to, and in fact also explains, (90).

Example 4.37. A final example is to (briefly) revisit the torus links through Theorem 4.35. When $L = T_{m,n}$, then $\lambda(K_i) = \alpha$ in (86). Thus $\phi = (\delta, \dots, \delta)$ from (71) is admissible. We checked (essentially because of (74)) that ϕ gives a banding with P -increasing flags. Then from Theorem 2.34 we have

$$\max \deg_v P(L(\phi)) = 2n - 1, \quad \min \deg_v [P(L(\phi))]_{z^{1-2l}} = 1 - 2m,$$

yielding $\ell_\phi(L) = m + n$, as before.

Acknowledgement

We are grateful to Andrey Morozov for a useful discussion. The work of A.M. was partially funded within the state assignment of the Institute for Information Transmission Problems of RAS, was partly supported by the grant of the Foundation for the Advancement of Theoretical Physics and Mathematics “BASIS” and by Armenian SCS grants 24WS-1C031. The work of H.S. and V.K.S. is supported by Tamkeen UAE under the NYU Abu Dhabi Research Institute grant CG008.

References

- [Al] J. W. Alexander, *Topological invariants of knots and links*, Trans. Amer. Math. Soc. **30** (1928), 275–306, [doi:10.1090/S0002-9947-1928-1501429-1].
- [AHT] T. Ando, C. Hayashi, and M. Taguchi, *Cromwell moves on grid diagrams for knots and links*, preprint.
- [AM] A. Anokhina and An. Morozov, *Cabling procedure for the colored HOMFLY polynomials*, Teor. Mat. Fiz. **178** (2014), 3–68, [doi:10.1007/s11232-014-0129-2], [arXiv:1307.2216].
- [Be] D. Bennequin, *Entrelacements et équations de Pfaff*, Soc. Math. de France, Astérisque **107-108** (1983), 87–161, [numdam.org/item/AST_1983_107-108_87_0].
- [BKL] J. S. Birman, K. Ko, and S. J. Lee, *A new approach to the word and conjugacy problems in the braid groups*, Adv. Math. **139**(2) (1998), 322–353, [doi:10.1006/aima.1998.1761].
- [BMe] J. S. Birman and W. W. Menasco, *Studying links via closed braids II: On a theorem of Bennequin*, Topology Appl. **40**(1) (1991), 71–82, [doi:10.1016/0166-8641(91)90059-U].
- [BMi] L. Bishler and A. Mironov, *Torus knots in adjoint representation and Vogel’s universality*, Eur. Phys. J. **C85** (2025) 8, 911, [doi:10.1140/epjc/s10052-025-14651-7], [arXiv:2506.06219].
- [BD] B. Bode and M. R. Dennis, *Constructing a polynomial whose nodal set is any prescribed knot or link*, J. Knot Theory Ramif. **28** (2019), 1850082, [doi:10.1142/S0218216518500827].
- [BO] M. Boileau and S. Orevkov, *Quasi-positivité d’une courbe analytique dans une boule pseudo-convexe*, C. R. Acad. Sci. Paris **332** (2001), 1–6, [doi:10.1016/S0764-4442(01)01945-0].
- [ChE] I. Cherednik and R. Elliot, *Refined composite invariants of torus knots via DAHA*, Ann. Fac. Sci. Toulouse Math. **25** (2016), 433–471, [doi:10.5802/afst.1501], [arXiv:1503.01441].

[D+] S. Dhara, A. Mironov, A. Morozov, An. Morozov, P. Ramadevi, V. K. Singh, and A. Sleptsov, *Multi-Colored Links From 3-strand Braids Carrying Arbitrary Symmetric Representations*, Ann. Henri Poincaré **20**(12) (2019), 4033–4054, [doi:10.1007/s00023-019-00841-z], [arXiv:1805.03916].

[DM] Y. Diao and H. Morton, *The braid indices of the reverse parallel links of alternating knots*, Algebr. Geom. Topol. **24** (2024), 2957–2970, [doi:10.2140/agt.2024.24.2957].

[DP] I. A. Dynnikov and M. V. Prasolov, *Bypasses for rectangular diagrams. A proof of the Jones conjecture and related questions*, Trans. Moscow Math. Soc. **2013**, 97–144, [doi:10.1090/S0077-1554-2014-00210-7].

[EH] J. Etnyre and K. Honda, *Knots and Contact Geometry I: Torus Knots and the Figure Eight Knot*, J. Symp. Geom. **1**(1) (2001), 63–120, [Euclid: jsg/1092316299].

[FLL] P. Feller, L. Lewark, and A. Lobb, *Almost positive links are strongly quasipositive*, Math. Ann. **385** (2023), 481–510, [doi:10.1007/s00208-021-02328-x].

[FW] J. Franks and R. Williams, *Braids and the Jones polynomial*, Trans. Amer. Math. Soc. **303**(1) (1987), 97–108, [doi:10.1090/S0002-9947-1987-0896009-2].

[H+] P. Freyd, J. Hoste, W. Lickorish, K. Millet, A. Ocneanu, and D. Yetter, *A new polynomial invariant of knots and links*, Bull. Amer. Math. Soc. **12** (1985), 239–246, [doi:10.1090/S0273-0979-1985-15361-3].

[FT] D. Fuchs and S. Tabachnikov, *Invariants of Legendrian and transverse knots in the standard contact space*, Topology **36**(5) (1997), 1025–1053, [doi:10.1016/S0040-9383(96)00035-3].

[HM] R. Hadji and H. Morton, *A basis for the full HOMFLY skein of the annulus*, Math. Proc. Camb. Philos. Soc. **141** (2006), 81–100, [doi:10.1017/S0305004105009047].

[HS] M. Hirasawa and A. Stoimenov, *Examples of knots without minimal string Bennequin surfaces*, Asian J. Math. **7** (2003), 435–446, [doi:10.4310/AJM.2003.v7.n3.a6].

[JLS1] G. T. Jin, H. J. Lee, and A. Stoimenov, *Grid diagrams, link indices, and strong quasipositivity*, available at [stoimenov.net/stoimenov/homepage/papers.html].

[JLS2] G. T. Jin, H. J. Lee, and A. Stoimenov, *Grid diagrams, link indices, and the HOMFLY-PT polynomial*, available at [stoimenov.net/stoimenov/homepage/papers.html].

[Jo] V. Jones, *A polynomial invariant for knots via von Neumann algebras*, Bull. Amer. Math. Soc. (N.S.) **12** (1985), 103–111, [doi:10.1090/S0273-0979-1985-15304-2].

[KRT] C. Kassel, M. Rosso, and V. Turaev, *Quantum Groups and Knot Invariants*, Soc. Math. France, Paris (1997), [ISBN: 2-85629-055-8].

[KR] A. N. Kirillov and N. Reshetikhin, *The Bethe Ansatz and the combinatorics of Young tableaux*, J. Soviet Math. **41** (1988), 925–955, [doi:10.1007/BF01247088].

[KS] A. Klimyk and K. Schmüdgen, *Quantum Groups and Their Representations*, Texts and Monographs in Physics, Springer-Verlag, Berlin (1997), [doi:10.1007/978-3-642-60896-4].

[Ko] K. Koike, *On the decomposition of tensor products of the representations of the classical groups: by means of the universal characters*, Adv. Math. **74** (1989), 57–86, [doi:10.1016/0001-8708(89)90004-2].

[LM] W. B. R. Lickorish and K. C. Millett, *A polynomial invariant of oriented links*, Topology **26**(1) (1987), 107–141, [doi:10.1016/0040-9383(87)90025-5].

[LZ] X. S. Lin and H. Zheng, *On the Hecke algebras and the colored HOMFLY polynomial*, Trans. Amer. Math. Soc. **362**(1) (2010), 1–18, [doi:10.1090/S0002-9947-09-04691-1], [arXiv:math/0601267].

[LN] C. Livingston and S. Naik, *Ozsváth-Szabó and Rasmussen invariants of doubled knots*, Algebr. Geom. Topol. **6** (2006), 651–657, [doi:10.2140/agt.2006.6.651].

[Mac] I. G. Macdonald, *Symmetric Functions and Hall Polynomials*, Clarendon Press, Oxford (1995), [ISBN: 9780198504504].

[MMM] A. Mironov, R. Mkrtchyan, and A. Morozov, *On universal knot polynomials*, J. High Energy Phys. **02** (2016) 078, [[doi:10.1007/JHEP02\(2016\)078](https://doi.org/10.1007/JHEP02(2016)078)], [[arXiv:1510.05884](https://arxiv.org/abs/1510.05884)].

[MM] A. Mironov and A. Morozov, *On the Hopf-Induced Deformation of a Topological Locus*, JETP Lett. **107(11)** (2018), 728–735, [[doi:10.1134/S0021364018110048](https://doi.org/10.1134/S0021364018110048)], [[arXiv:1804.10231](https://arxiv.org/abs/1804.10231)].

[MMM2] A. Mironov, A. Morozov, and An. Morozov, *Character expansion for HOMFLY polynomials. II. Fundamental representation. Up to five strands in braid*, J. High Energy Phys. **03** (2012) 034, [[doi:10.1007/JHEP03\(2012\)034](https://doi.org/10.1007/JHEP03(2012)034)], [[arXiv:1112.2654](https://arxiv.org/abs/1112.2654)].

[Mo] H. R. Morton, *Seifert circles and knot polynomials*, Proc. Camb. Phil. Soc. **99** (1986), 107–109, [[doi:10.1017/S0305004100063982](https://doi.org/10.1017/S0305004100063982)].

[MB] H. R. Morton and E. Beltrami, *Arc index and the Kauffman polynomial*, Math. Proc. Cambridge Philos. Soc. **123** (1998), 41–48, [[doi:10.1017/S0305004197002090](https://doi.org/10.1017/S0305004197002090)].

[Na] T. Nakamura, *Notes on the braid index of closed positive braids*, Topology Appl. **135(1-3)** (2004), 13–31, [[doi:10.1016/S0166-8641\(03\)00109-3](https://doi.org/10.1016/S0166-8641(03)00109-3)].

[Nu] I. J. Nutt, *Embedding knots and links in an open book III. On the braid index of satellite links*, Math. Proc. Camb. Phil. Soc. **126** (1999), 77–98, [[doi:10.1017/S0305004198002849](https://doi.org/10.1017/S0305004198002849)].

[Re] K. Reidemeister, *Elementare Begründung der Knotentheorie*, Abh. Math. Semin. Univ. Hambg. **5** (1927), 24–32, [[doi:10.1007/BF02952507](https://doi.org/10.1007/BF02952507)].

[RT] N.Y. Reshetikhin, and V. G. Turaev, *Ribbon graphs and their invariants derived from quantum groups*, Commun. Math. Phys. **127(1)** (1990), 1–26, [[doi:10.1007/BF0120037](https://doi.org/10.1007/BF0120037)].

[RJ] M. Rosso and V. Jones, *On the invariants of torus knots derived from quantum groups*, J. Knot Theor. Ramifications **2** (1993), 97–112, [[doi:10.1142/S0218216593000064](https://doi.org/10.1142/S0218216593000064)].

[Ru1] L. Rudolph, *Knot theory of complex plane curves*, in *Handbook of Knot Theory*, W. Menasco and M. Thistlethwaite (eds.), Elsevier Science (2005), 329–428, [doi.org/10.1016/B978-044451452-3/50009-5].

[Ru2] L. Rudolph, *Braided surfaces and Seifert ribbons for closed braids*, Comment. Math. Helv. **58** (1983), 1–37, [[doi:10.1007/BF02564622](https://doi.org/10.1007/BF02564622)].

[Ru3] L. Rudolph, *An obstruction to sliceness via contact geometry and “classical” gauge theory*, Invent. Math. **119(1)** (1995), 155–163, [[doi:10.1007/BF01245177](https://doi.org/10.1007/BF01245177)].

[St1] A. Stoimenov, *Grid diagrams, link indices, and quasipositivity*, available at request from the author.

[St2] A. Stoimenov, *Realizing strongly quasipositive links and Bennequin surfaces*, to appear in Publ. Res. Inst. Math. Sci., [stoimenov.net/stoimenov/homepage/papers.html].

[St3] A. Stoimenov, *Diagram genus, generators and applications*, T&F/CRC Press Monographs and Research Notes in Mathematics (2016), [[doi:10.1201/9781315368672](https://doi.org/10.1201/9781315368672)].

[St4] A. Stoimenov, *Sublinks of strongly quasipositive links*, J. Math. Sci. (Series B), **275(1)** (2023), 38–54, [[doi:10.1007/s10958-023-06658-w](https://doi.org/10.1007/s10958-023-06658-w)].

[Ta1] T. Tanaka, *Maximal Thurston-Bennequin numbers of alternating links*, Topology Appl. **153(14)** (2006), 2476–2483, [[doi:10.1016/j.topol.2005.10.001](https://doi.org/10.1016/j.topol.2005.10.001)].

[Ta2] T. Tanaka, *Maximal Bennequin numbers and Kauffman polynomials of positive links*, Proc. Amer. Math. Soc. **127(11)** (1999), 3427–3432, [[doi:10.1090/S0002-9939-99-04983-7](https://doi.org/10.1090/S0002-9939-99-04983-7)].